

University of Texas at Tyler

## Scholar Works at UT Tyler

---

Biotechnology Theses

Biotechnology

---

Spring 6-9-2023

# EFFECTS OF INTERLEUKIN-22 (IL-22) ON NECROPTOSIS, INFLAMMATORY RESPONSES, AND METABOLISM OF MYCOBACTERIUM TUBERCULOSIS STIMULATED TYPE 2 DIABETES MELLITUS MOUSE MACROPHAGES

Bismark Owusu-Afriyie

University of Texas Health Center at Tyler, bowusuafriyie@patriots.uttyler.edu

Follow this and additional works at: [https://scholarworks.uttyler.edu/biotech\\_grad](https://scholarworks.uttyler.edu/biotech_grad)



Part of the Biotechnology Commons, Medical Biotechnology Commons, Medical Immunology Commons, Medical Microbiology Commons, and the Medical Pharmacology Commons

---

### Recommended Citation

Owusu-Afriyie, Bismark, "EFFECTS OF INTERLEUKIN-22 (IL-22) ON NECROPTOSIS, INFLAMMATORY RESPONSES, AND METABOLISM OF MYCOBACTERIUM TUBERCULOSIS STIMULATED TYPE 2 DIABETES MELLITUS MOUSE MACROPHAGES" (2023). *Biotechnology Theses*. Paper 10.  
<http://hdl.handle.net/10950/4230>

This Thesis is brought to you for free and open access by the Biotechnology at Scholar Works at UT Tyler. It has been accepted for inclusion in Biotechnology Theses by an authorized administrator of Scholar Works at UT Tyler. For more information, please contact [tgullings@uttyler.edu](mailto:tgullings@uttyler.edu).

EFFECTS OF INTERLEUKIN-22 (IL-22) ON NECROPTOSIS, INFLAMMATORY  
RESPONSES, AND METABOLISM OF *MYCOBACTERIUM TUBERCULOSIS*  
STIMULATED TYPE 2 DIABETES MELLITUS MOUSE MACROPHAGES

by

BISMARK OWUSU-AFRIYIE

A thesis submitted in partial fulfillment of  
the requirements for the degree of  
Master of Science in Biotechnology  
Department of Cellular and Molecular Biology

Ramakrishna Vankayalapati, Ph.D., Thesis Advisor

School of Medicine

The University of Texas at Tyler  
April 2023

The University of Texas at Tyler  
Tyler, Texas

This is to certify that the Master Thesis of

BISMARCK OWUSU-AFRIYIE

has been approved for the thesis requirement on  
April 20, 2023, for  
the Master of Science in Biotechnology degree

Approvals:



Thesis Advisor: Ramakrishna Vankayalapati, Ph.D.



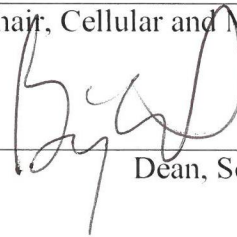
Committee Chair: Vijay Boggaram, Ph.D.



Member: Buka Samten, M.D.



Chair, Cellular and Molecular Biology



Dean, School of Medicine

## ACKNOWLEDGMENTS

Words cannot express my gratitude to my thesis advisor, Professor Ramakrishna Vankayalapati, for his patience and guidance. This endeavor would not have been possible without the invaluable feedback from Professor Vijay Boggaram, who was my thesis committee chairman, and Professor Buka Samten, my thesis committee member. I could not have undertaken this journey without Research Assistant Professor Rajesh Kumar Radhakrishnan, who generously provided knowledge and expertise.

I had the pleasure of working with wonderful people throughout my research. Many thanks to my laboratory members especially Olamipejo Durojaye, Tanmoy Mukherjee and Oyinkansola Faith Adeyemi for their immeasurable support. I would be remiss in not mentioning Professor Torry Tucker, Professor Pierre Neuenschwander, Professor Amy Tvinnereim, and Professor Mitsuo Ikebe for their advice and suggestion throughout my studies. Additionally, this endeavour would not have been possible without the generous funding by the Biotechnology Program, the support of the program coordinators and all administrative staff. I thank my classmates and all MS Biotechnology students of UT Tyler Health Science Center from 2021 to 2023. They impacted and inspired me.

Finally, special thanks and recognition goes to my former professors and my family, especially my wife (Mrs. Louisa Pokua Owusu-Afriyie), my two daughters (Nanayaa and Awurabena) and my mother (Elizabeth Gyamfi). Their belief in me motivated me during my studies. I can never forget their emotional support. Thanks should also go to Mr. Peter Owusu and the Ghanaian community in Tyler for supporting my stay in the city.

## TABLE OF CONTENTS

Table of Contents .....	i
LIST OF FIGURES .....	iv
LIST OF TABLES .....	vi
LIST OF ABBREVIATIONS.....	vii
ABSTRACT.....	x
INTRODUCTION .....	1
RESEARCH HYPOTHESIS .....	3
MATERIALS AND METHODS.....	4
Materials and Stock Solutions.....	4
Reagent Preparation .....	5
Animals .....	6
Type 2 Diabetes Mellitus Induction.....	6
Isolation and Culture of Mouse Lung and Peritoneal Macrophages.....	7
Flow cytometry .....	9
Lactate Dehydrogenase Assay .....	10
Western Blot .....	10
Enzyme-Linked Immunosorbent Assay (ELISA).....	10
Metabolism Assay.....	11

Statistical Analysis.....	11
RESULTS .....	12
Previous study from the laboratory .....	12
AIM 1: Determine whether IL-22 inhibits necroptosis of <i>Mtb</i> -stimulated macrophages of T2DM mice.....	12
Body weight of mice .....	13
Blood glucose levels of the mice .....	14
Purity of isolated lung macrophages .....	15
Purity of isolated peritoneal macrophages .....	15
Recombinant IL-22 had no effect on the viability of lung and peritoneal macrophages .	16
Recombinant IL-22 inhibits the expression of necroptotic marker pMLKL by <i>Mtb</i> -cultured T2DM mice lung macrophages.....	19
Recombinant IL-22 has no effect on TNF- $\alpha$ and IL-6 production by $\gamma$ <i>Mtb</i> -cultured T2DM mice macrophages.....	21
AIM 2: Determine whether IL-22 regulates metabolism (glycolysis and oxidative phosphorylation) of <i>Mtb</i> -stimulated macrophages from T2DM mice.....	23
Recombinant IL-22 has no effect on oxidative phosphorylation of $\gamma$ <i>Mtb</i> -cultured T2DM mice peritoneal macrophages.....	23
Recombinant IL-22 has no effect on the extracellular acidification rate of $\gamma$ <i>Mtb</i> -stimulated peritoneal macrophages from T2DM mice .....	25

Recombinant IL-22 has no effect on the extracellular acidification rate of $\gamma$ <i>Mtb</i> -stimulated lung macrophages from T2DM mice .....	26
DISCUSSION.....	28
REFERENCES .....	33
Supplementary Materials .....	41
VITA.....	43

## LIST OF FIGURES

Figure 1. NA/STZ injection reduces body weight and increases blood glucose levels of C57BL/6 wild-type female mice.....	13
Figure 1. NA/STZ injection reduces body weight and increases blood glucose levels of C57BL/6 wild-type female mice.....	13
Figure 2. Representative flow cytometry demonstrating the purity of the isolated alveolar and peritoneal macrophages. ....	16
Figure 2. Representative flow cytometry demonstrating the purity of the isolated alveolar and peritoneal macrophages. ....	16
Figure 3. Recombinant interleukin-22 has no effect on viability of $\gamma$ Mtb-cultured macrophages. ....	18
Figure 3. Recombinant interleukin-22 has no effect on viability of $\gamma$ Mtb-cultured macrophages. ....	18
Figure 4. Recombinant IL-22 reduces expression of pMLKL protein in $\gamma$ -irradiated Mtb-stimulated mice lung macrophages of T2DM mice.....	20
Figure 4. Recombinant IL-22 reduces expression of pMLKL protein in $\gamma$ -irradiated Mtb-stimulated mice lung macrophages of T2DM mice.....	20
Figure 5. Recombinant IL-22 reduces expression of pRIPK3 and pMLKL proteins in $\gamma$ Mtb-stimulated peritoneal macrophages of T2DM mice.....	21
Figure 5. Recombinant IL-22 reduces expression of pRIPK3 and pMLKL proteins in $\gamma$ Mtb-stimulated peritoneal macrophages of T2DM mice.....	21
Figure 6. Recombinant IL-22 has no effect on TNF- $\alpha$ and IL-6 production by $\gamma$ Mtb-stimulated macrophages of T2DM mice.....	22



Figure 6. Recombinant IL-22 has no effect on TNF- $\alpha$ and IL-6 production by $\gamma$ Mtb-stimulated macrophages of T2DM mice.....	22
Figure 7. Recombinant IL-22 has no effect on oxidative phosphorylation of $\gamma$ Mtb-stimulated peritoneal macrophages of T2DM mice. ....	24
Figure 7. Recombinant IL-22 has no effect on oxidative phosphorylation of $\gamma$ Mtb-stimulated peritoneal macrophages of T2DM mice. ....	24
Figure 8. Recombinant IL-22 has no effect on extracellular acidification rate of $\gamma$ Mtb-stimulated peritoneal macrophages.....	25
Figure 8. Recombinant IL-22 has no effect on extracellular acidification rate of $\gamma$ Mtb-stimulated peritoneal macrophages.....	25
Figure 9. Recombinant IL-22 has no effect on extracellular acidification rate of $\gamma$ Mtb-stimulated lung macrophages from T2DM mice. ....	27
Supplementary Figure 1. Recombinant IL-22 has no effect on TNF- $\alpha$ , IL-6 and IFN- $\gamma$ production by $\gamma$ Mtb-stimulated macrophages of T2DM mice.....	41
Supplementary Figure 2. Effect of recombinant IL-22 on total MLKL protein expression by T2DM mice lung macrophages stimulated with $\gamma$ -irradiated <i>Mtb</i> .....	42

## LIST OF TABLES

Table 1. Cell surface markers, fluorophores and channels for checking the purity of isolated cells .....	9
--	---

## LIST OF ABBREVIATIONS

**BSA:** Bovine Serum Albumin

**EDTA:** Etheylenediaminetetra-acetic Acid

**TNF- $\alpha$ :** Tumor Necrosis Factor Alpha

**DMEM:** Dulbecco's Modified Eagle's Medium

**IL-6:** Interleukin-6

**IL-22:** Interleukin-22

**ELISA:** Enzyme-linked Immunosorbent Assay

**LDH:** Lactate Dehydrogenase

**T2DM:** Type-2 Diabetes Mellitus

**PBS:** Phosphate-buffered Saline

**PBST:** Phosphate-buffered Saline Tween

**HBSS:** Hank's Balanced Salt Solution

**RPMI:** Roswell Park Memorial Institute

**FBS:** Fetal Bovine Serum

**MACS:** Magnetic-activated Cell Sorting

**TLR3:** Toll-like Receptor 3

**TLR4:** Toll-like Receptor 4

**TNFR1:** Tumor Necrosis Factor Receptor 1

**RIPK1:** Receptor Interacting Protein Kinase 1

**pRIPK1:** Phosphorylated Receptor Interacting Protein Kinase 1

**RIPK3:** Receptor Interacting Protein Kinase 3

**pRIPK3:** Phosphorylated Receptor Interacting Protein Kinase 3

**MLKL:** Mixed Lineage Kinase Domain-like Protein

**pMLKL:** Phosphorylated Mixed Lineage Kinase Domain-like Protein

**GAPDH:** Glyceraldehyde-3-phosphate Dehydrogenase

*Mtb:* *Mycobacterium tuberculosis*

**TB:** Tuberculosis

**LTBI:** Latent Tuberculosis Infection

**NIH:** National Institute of Health

**OLAW:** Office of Laboratory Animal Welfare

**NA:** Nicotinamide

**STZ:** Streptozotocin

**RBG:** Random blood glucose

**PCR:** Polymerase Chain Reaction

**qRT-PCR:** Quantitative Real-time Polymerase Chain Reaction

**RNA:** Ribonucleic Acid

**ATP:** Adenosine Triphosphate

**FACS:** Florescence-activated Cell Sorting

## ABSTRACT

*Mycobacterium tuberculosis* (*Mtb*) infects one-third of the world's population and causes nearly 1.3 million deaths per year. Limited information is available about the immune responses during *Mtb* infection in type 2 diabetic hosts. Our laboratory developed an experimentally induced type 2 diabetes (T2DM) model in wild-type C57BL/6 mice and found that IL-22 and type 3 innate lymphoid cells (ILC3s) reduce inflammation and mortality of *Mtb*-infected T2DM mice. Our laboratory also found that *Mtb*-infected alveolar macrophages (AMs) from T2DM mice undergo necroptosis compared to *Mtb*-infected AMs of non-T2DM mice. In the current study, we determined whether recombinant IL-22 treatment of  $\gamma$ *Mtb*-stimulated macrophages of T2DM mice inhibits the expression of necroptosis, reduces inflammatory cytokine production, and regulates the metabolism of the macrophages. We found that  $\gamma$ *Mtb* stimulation of T2DM mice lung macrophages significantly enhanced the expression of necroptotic markers such as pMLKL (phosphorylated pseudokinase mixed lineage kinase domain-like protein) compared to  $\gamma$ *Mtb*-stimulated lung macrophages of non-diabetic mice. Recombinant IL-22 treatment significantly inhibited the expression of pMLKL by  $\gamma$ *Mtb* stimulated lung macrophages of T2DM mice. The treatment marginally reduced the glycolytic parameters of these macrophages. However, the treatment had no effect on pro-inflammatory cytokines (IL-6 and TNF- $\alpha$ ) production by  $\gamma$ *Mtb*-stimulated macrophages of T2DM mice. In future studies, live *Mtb* H37Rv will be used to infect macrophages to determine cell viability and necroptosis. Further understanding of the mechanisms involved in IL-22-mediated inhibition of pMLKL will help to develop therapies to prevent excess inflammation in T2DM individuals with active and latent tuberculosis infection.

## INTRODUCTION

*Mycobacterium tuberculosis* (Mtb) is an airborne disease and infects one-third of the human population [1] and it remains a leading cause of mortality worldwide [2], [3]. Most of the Mtb-infected people develop latent tuberculosis infection (LTBI) and remain asymptomatic [4]. There is a high risk of LTBI reactivation in persons with immuno-compromising morbidities such as HIV/AIDS, cancer, alcoholism, smoking, malnutrition and diabetes mellitus (DM) [5]. Type 2 diabetes mellitus (T2DM) is the most prevalent comorbidity among patients with tuberculosis [6], [7].

Diabetes is a chronic metabolic disorder characterized by persistently raised glycemia as a result of defects in insulin sensitivity and/or secretion [8]. It was estimated that 463 million people worldwide had diabetes in 2019 and this prevalence is expected to increase by 25% in 2030 and further rise by 51% in 2045. Recent meta-analysis suggested a two- to four-fold increased risk of association between active tuberculosis and diabetes [5].

The immune mechanisms which lead to the increased susceptibility of T2DM patients to Mtb are largely due to defects in bacterial recognition, phagocytic activity and cellular activation of macrophages [9], [10]. T2DM impairs the production of cytokines and chemokines, recruitment and function of antigen-presenting cells as well as initiation of adaptive immunity [9]. However, a detailed understanding of the protective immune responses in T2DM hosts during Mtb infection is essential to develop an effective prophylactic or therapeutic agent.

Previously, our laboratory developed an experimentally induced T2DM model in wild-type C57BL/6 mice and found that Mtb infection in T2DM mice drives pathological immune responses and mortality [11]. The laboratory also found F4/80+CD11c+ alveolar macrophages (AMs) from

*Mtb*-infected T2DM mice are less apoptotic; produce more IL-6; express higher levels of tumor necrosis factor receptor 1 (TNFR1), phosphorylated receptor-interacting kinase proteins (pRIPK1, pRIPK3), and mixed-lineage kinase domain-like (MLKL); and are more necroptotic compared to *Mtb*-infected AMs of non-T2DM mice [unpublished data]. Among various pro- and anti-inflammatory cytokines measured in *Mtb*-infected T2DM mice, only IL-22 levels were significantly reduced when compared to non-diabetic *Mtb*-infected mice [12]. Further studies demonstrated that recombinant IL-22 reduces mortality of T2DM mice [12], [13].

IL-22 is a member of IL-10 family of cytokines which is secreted by T cells,  $\gamma\delta$ T cells and natural killer cells [13]. IL-22 contributes to immunity against TB by enhancing phagosomal maturation of macrophages and reducing intracellular growth of mycobacteria in macrophages [14]–[16]. IL-22 regulates glucose homeostasis [17], [18] and excess inflammation and plays an important role in controlling infections, including *Mtb*, suggesting the IL-22 pathway as a novel target for therapeutic intervention [11], [12], [14].

In the current study, we investigated mechanisms by which IL-22 regulates enhanced inflammatory responses and necroptosis of gamma *Mtb*-stimulated macrophages of T2DM mice. We determined whether recombinant IL-22 (rIL-22) treatment of  $\gamma$ *Mtb*-stimulated macrophages of T2DM mice inhibits expression of necroptotic marker pMLKL and inflammatory cytokine production. We also determined whether rIL-22 regulates the metabolism (glycolysis and oxidative phosphorylation) of  $\gamma$ *Mtb*-stimulated macrophages of T2DM mice.



## RESEARCH HYPOTHESIS

**Recombinant IL-22 treatment regulates necroptotic signaling and reduces inflammatory responses of T2DM mice macrophages stimulated with  $\gamma$ *Mtb*. IL-22 helps to maintain homoeostatic glycolysis of  $\gamma$ *Mtb*-stimulated T2DM mice macrophages to reduce necroptosis and inflammation.**

### **Specific Aims:**

**Aim 1:** Determine whether rIL-22 inhibits necroptosis of *Mtb*-stimulated T2DM mice macrophages.

**Aim 2:** Determine whether rIL-22 regulates metabolism (glycolysis and oxidative phosphorylation) of *Mtb*-stimulated macrophages from T2DM mice.

## MATERIALS AND METHODS

### Materials and Stock Solutions

Deionized water, 10X Phosphate-buffered saline (PBS; SIGMA<sup>®</sup>), 1X pharmaceutical grade PBS (VWR), CO<sub>2</sub> chamber, mice organ harvesting table, aluminum foil, streptozotocin (Cayman chemical company), nicotinamide (SIGMA<sup>®</sup>), weight scale (ADAM), glucometer (Contour next ONE), 0.2 mg/ml mouse recombinant IL-22 (BioLegend), 1X Hank's balanced salt solution (HBSS; Lonza), Gamma irradiated-*Mtb* (NIH), collagenase A (Roche), dispase (Fisher Scientific), DNASE 1 (Fisher Scientific), 40 µm nylon mesh (Fisherbrand), petri dishes (Fisherbrand), mouse Anti-F4/80 UltraPure MicroBeads (Miltenyi Biotec), magnetic-activated cell sorting (MACS) separation columns (Miltenyi Biotec), 0.4% Trypan blue solution (Amresco), microscope (Olympus), 1X Roswell Park Memorial Institute media (Corning), 1% penicillin (Fisher Scientific), 10% fetal bovine serum (Fisher Scientific), bovine serum albumin (Fisher bioreagents), Nalgen<sup>™</sup> rapid flow filter unit (Thermo Scientific), 37°C incubator with 5% CO<sub>2</sub>, 37°C water bath, 4°C and -80°C refrigerators, Phosphate-buffered saline tween (PBST) buffer powder (QuickSILVER); glycolysis stress test kit (Agilent Technologies), mito stress test kit (Agilent Technologies), Seahorse XFe96 analyzer (Agilent Technologies), XFe96 cell culture and running plates (Agilent Technologies), pipettes with matching sterile tips, 24-well cell culture plates, 70% EtOH, conical tubes, mouse IL-6, TNF- $\alpha$  and IFN- $\gamma$  ELISA kits (BioLegend<sup>®</sup>), microcentrifuge (Thermo Scientific), vortex (Scientific Industries), mouse primary anti-bodies for western blot (pRIPK3, total RIPK3, pMLKL (Sigma), total MLKL and  $\beta$ -actin (Cell Signaling Technology and Santa Cruz Biotechnology), methanol (Fisher chemical), anti-mouse and anti-rabbit HRP-linked secondary antibodies (Cell Signaling Technology), non-fat milk powder (LabScientific Inc.), EveryBlot blocking buffer (Bio-Rad), stripping buffer (PIERCE),

ChemiDoc™ Imaging System (Bio-Rad), 1% paraformaldehyde (Millipore Sigma), Attune NxT acoustic flow cytometer (Invitrogen), FACS tubes, LIVE/DEAD fixable aqua dead cell stain kit (Invitrogen), cell surface markers (CD45, F4/80, Siglec F, CD11b; BioLegend®), CyQUANT™ LDH Cytotoxicity Assay kit (Thermo Fisher), western blot gels (Invitrogen), mini gel tank (Invitrogen), blot transfer tank (Bio-Rad), M-PER™ mammalian protein extraction reagent (Thermo Scientific), Halt™ protease and phosphatase inhibitor (Thermo Scientific), Pierce BCA protein assay kit (ThermoFisher Scientific), Clarity Max™ western enhanced chemiluminescence substrate (Bio-Rad), 1X running buffer (Bio-Rad), 1X transfer buffer (Bio-Rad), precision plus protein standard (Bio-Rad), hotplate/stirrer (VWR) and orbital shaker (Bellco Biotechnology).

#### Reagent Preparation

- a. Streptozotocin was dissolved in sterile 1X PBS (pharmaceutical grade) to a final concentration of 50.0 mg/ml.
- b. Nicotinamide was dissolved in sterile 1X PBS (pharmaceutical grade) to a final concentration of 20.0 mg/ml.
- c. Mouse rIL-22 was diluted with sterile 1X HBSS to a final concentration of 5 µg/ml.
- d. RPMI-1640 complete cell culture media (CRPMI-1640) supplemented with 1% penicillin/streptomycin and 10% heat inactivated fetal bovine serum. The medium was filtered using Nalgene™ rapid flow filter unit (0.2 µm) and stored at 4°C.
- e. Magnetic-activated cell sorting (MACS) buffer was composed of 0.5% BSA and 0.2% of 0.5 mM EDTA in 1X PBS.
- g. 1X PBST was prepared by adding 1L deionized water to one sachet of PBST buffer powder. It was then stirred until the powder completely dissolved.

h. Mitochondrial stress test assay media: 1% glutamine, 1% pyruvate and 1% glucose in Seahorse DMEM media.

i. Glycolysis stress test assay media: 1% glutamine in Seahorse DMEM media.

j. Enzyme-tissue digestion buffer: 0.25% collagenase A, 20% dispase, 1.25% DNASE 1 in 1X RPMI.

### Animals

Specific pathogen-free 4- to 6-week-old female C57BL/6 mice were purchased from the Jackson Laboratory and housed at the animal facility at the University Texas at Tyler Health Science Center. All animal studies were approved by the Institutional Animal Care and Use Committee of the University of Texas at Tyler Health Science Center (protocol #717). The animal procedures involving the care and use of mice were carried out in accordance with the guidelines of the NIH/OLAW (Office of Laboratory Animal Welfare). Gamma-irradiated *Mtb* was used to stimulate macrophages (in vitro) throughout this study.

### Type 2 Diabetes Mellitus Induction

Type-2 diabetes mellitus (T2DM) was induced by combined administration of Streptozotocin (STZ) and Nicotinamide (NA) as described previously [11], [12]. In brief, STZ was administered (180 mg/kg of body weight) intraperitoneally (i.p.) 3 times, with an interval of 10 days between doses. NA was administered i.p. (60 mg/kg of body weight) 15 minutes before the STZ injections. Control mice received only sterile pharma-grade PBS injections. The body weight of both PBS- and NA/STZ-injected mice were taken at the same time points on the first day of injection and every other 10- or 15-days afterwards up to 150 days using the same weight scale.

Where the tenth or fifteenth day was a Saturday or Sunday, the weight was taken on a day before or after (that is, the preceding Friday or the next Monday).

After one month of the third dose of PBS- and NA/STZ-injections, one mouse was randomly selected from each cage and their random blood glucose (RBG) levels were measured at the same time point using a glucometer to confirm the induction of diabetes before commencing the study. Thereafter, the RBG levels of mice were measured using the same glucometer and at the same time (between 9:00am and 10:30am) before euthanizing them for experiments. Induction of diabetes was confirmed by a significant increase in RBG in the NA/STZ-treated mice [19].

#### Isolation and Culture of Mouse Lung and Peritoneal Macrophages

Mice were euthanized by CO<sub>2</sub> asphyxiation followed by cervical dislocation. To obtain lung macrophages, an incision was made along the bottom midline of the peritoneum and the abdominal skin to expose the rib cage. The rib cage was then cut to expose the heart and lung. The lung of each mouse was perfused with 10 ml of sterile sterile PBS via the right ventricle of the heart. The lung was then harvested, cut into pieces and incubated in 500 µl enzyme-tissue digestion buffer at 37°C and 5% CO<sub>2</sub> for 30 minutes. It was then filtered through a 40 µm nylon cell strainer and HBSS was added to a final volume of 10 ml. Cells were separated from the buffer by centrifugation at 400 x g for 5 minutes. The supernatant was discarded, pellets washed with another 10 ml of HBSS and centrifuged again at 400 x g for 5 minutes. The supernatant was then discarded.

Murine lung macrophages were isolated from the cell pellets by magnetic-activated cell sorting (MACS) separation using Anti-F4/80 microbeads according to the manufacturer's protocol [20]. Briefly, the pellets from each lung were resuspended in 90 µl of MACS buffer and 15 µl of Anti-F4/80 microbeads was added and mixed thoroughly. It was then incubated for 15 minutes in the dark at 4°C. The cells were then washed by adding 2 ml of MACS buffer and centrifuged at

300 x g for 10 minutes. The supernatant was discarded, and the cells were resuspended in 3 ml of MACS buffer for magnetic separation using LS columns. Total lung (alveolar and interstitial) macrophages were separated by positive selection. Cells were resuspended in in RPMI-1640 complete media after centrifugation at 350 x g for 10 minutes. Cells were plated in 24-well cell culture plates at a density of 2.0 to 2.5 ×10<sup>5</sup> cells per well. Non-adherent cells were removed by washing the plate twice with normal HBSS followed by CRPMI-1640 media after 14- to 16- hours.

For isolation of mouse peritoneal macrophages, mice were euthanized by CO<sub>2</sub> asphyxiation followed by cervical dislocation. Subsequently, a small incision was made along the bottom midline of the peritoneum, and the abdominal skin was retracted to expose the transparent peritoneal skin. Peritoneal cells were collected by injecting 5 ml of ice-cold 1X PBS into the peritoneal cavity thrice using 27-gauge needle. The cells were then separated by centrifugation at 350 x g for 10 minutes, plated in 24-well tissue culture plates with CRPMI media at a density of 1 x 10<sup>6</sup> cells/well and incubated for 14 and 16 hours at 37 °C with 5% CO<sub>2</sub> to allow adherence of macrophages onto the plate. Non-adherent cells were removed by washing the plate twice with normal 1X HBSS followed by CRPMI media. The cell culture media was then replaced.

To obtain splenocytes, an incision was made along the bottom midline of the peritoneum and the abdominal skin. The spleen was then harvested, homogenized and filtered through a 40 μm nylon cell strainer and HBSS was added to a final volume of 10 ml. Cells were separated from the buffer by centrifugation at 350 x g for 10 minutes. The supernatant was discarded, pellets washed with another 10 ml of 10 ml of HBSS and centrifuged again at 350 x g for 10 minutes. The supernatant was then discarded, the cells were plated in 12-well tissue culture plates with CRPMI-1640 media and incubated for 14 hours at 37 °C with 5% CO<sub>2</sub>. Contaminants were removed by replacing the media after 14 hours.

For in vitro antigen stimulation experiments, cells were cultured with or without mouse recombinant IL-22 (10 ng/ml) and 10 µg/mL of  $\gamma$ -irradiated *Mtb* two hours after the rIL-22 stimulation and at 37°C and 5% CO<sub>2</sub> for 24, 48 or 72 hours. Cells were collected for mRNA expression analysis, flow cytometry staining, western blot, metabolic flux assay by seahorse and the culture supernatants were collected and stored at -80°C for cytotoxicity assay and cytokines analysis.

### Flow cytometry

This was performed to check the purity of the isolated macrophages. For surface staining, cultured cells were resuspended in 200 µL of sterile 1X PBS and a cocktail of 3 µL of each antibody (Table 1). The cells were incubated at 4°C for 30 minutes, washed twice with 1mL of the sterile 1X PBS at 350 x g for 5 minutes, and fixed in 1% paraformaldehyde before acquisition using an Attune NxT acoustic flow cytometer. Analysis was done using FlowJo version 10.8.1 software.

**Table 1. Cell surface markers, fluorophores and channels for checking the purity of isolated cells**

<b>Cell Surface Marker</b>	<b>Fluorophore</b>	<b>Channel on Attune Flow Cytometer</b>
LIVE/DEAD Fixable Aqua	Fixable Aqua	VL2
CD45	BV605	VL3
F4/80	BV421	VL1
Siglec F	PE/Dazzle 594	YL2
CD11b	PE/Cy 7	YL4

### Lactate Dehydrogenase Assay

Lung and peritoneal macrophages were cultured as mentioned above (pages 17-19). The cell culture supernatants were collected after 24- and 72- hours of stimulation and stored at  $-80^{\circ}\text{C}$ . Cytotoxicity levels were measured by CyQUANT<sup>TM</sup> LDH Cytotoxicity Assay according to the manufacturer's protocol [21]. The positive control from the manufacturer was used to determine the maximum cell death. The CRPMI-1640 culture media was used as a negative control and its absorbance was subtracted from that of each sample.

### Western Blot

Lung and peritoneal macrophages were cultured as mentioned above (pages 17-19). The pellets were collected after 72-hours and lysed using ice-cold 1X Halt<sup>TM</sup> protease and phosphatase inhibitor in M-PER<sup>TM</sup> mammalian protein extraction reagent. The lysate was collected into new tubes and incubated at  $4^{\circ}\text{C}$  with agitation for 30 minutes. It was then vortexed vigorously for 30 seconds, then centrifuged at  $350 \times g$  for 10 minutes at  $4^{\circ}\text{C}$ . The supernatant was then collected into new tubes and the protein was estimated using Pierce BCA assay according to the manufacturer's protocol [22]. The levels of pRIPK3, total RIPK3, pMLKL, total MLKL and  $\beta$ -actin were determined via western (immuno)-blotting according to the manufacturers' guidelines [23], [24]. Protein bands were quantified using Image J Software (NIH) and they were normalized to the respective  $\beta$ -actin.

### Enzyme-Linked Immunosorbent Assay (ELISA)

Lung and peritoneal macrophages were cultured as mentioned above (pages 17-19). Supernatants were collected after 24 hours of stimulation and stored at  $-80^{\circ}\text{C}$ . The concentrations



of tumor necrosis factor alpha (TNF- $\alpha$ ) and interleukin-6 (IL-6) were measured according to the manufacturer's protocol [25], [26].

#### Metabolism Assay

Lung and peritoneal macrophages were cultured as described previously in XF96 cell culture plates. Mitochondrial respiration assay and extracellular acidification assay were performed with Seahorse XFe96 analyzer after injection of glucose (1 mM), oligomycin (inhibitor of ATP synthase) (1.5  $\mu$ M), FCCP (an electron transport chain uncoupling agent) (1  $\mu$ M) plus sodium pyruvate (1 mM), rotenone/antimycin A (inhibitor of complex I/ inhibitor of complex III) (0.5  $\mu$ M) and 2-Deoxy-d-glucose (a competitive inhibitor of glucose) (5  $\mu$ M) according to the manufacturer's protocol [27], [28].

#### Statistical Analysis

Data analysis was carried out using GraphPad Prism version 9.3.1.471 (GraphPad Software Inc.) and all results were expressed as mean  $\pm$  standard error of the mean (SEM). Paired t-test was performed to compare the two groups of mice. One-way ANOVA followed by Tukey's test was used for comparison among samples.  $P < 0.05$  was considered statistically significant.

## RESULTS

### Previous study from the laboratory

Previously, our laboratory found that *Mtb* infection in T2DM mice enhances inflammatory cytokines (TNF- $\alpha$  and IL-6) production by CD11c<sup>+</sup> cells which drives pathological immune responses and mortality [11]. Further, we determined underlying mechanisms of enhanced inflammatory responses of AMs. Among various cell death pathways, we found necroptosis is major pathway involved in inflammatory cytokine production and TNFR1-dependent cell death of AMs. Anti-TNFR1 neutralizing antibody treatment of *Mtb*-infected AMs from T2DM mice significantly reduced the necroptosis gene expression (Rip1k and Rip3k) and inflammatory cytokines such as IL-6 levels. In addition, we also found that recombinant IL-22 treatment reduced the mortality and inflammation in T2DM mice infected with *Mtb* [12].

AIM 1: Determine whether IL-22 inhibits necroptosis of *Mtb*-stimulated macrophages of T2DM mice.

NA/STZ injection reduces the body weight and increases blood glucose levels of C57BL/6 wild-type female mice.

Induction of T2DM was shown in schematic diagram in Figure 1A.

## Body weight of mice

The body weight of both PBS- and NA/STZ-injected mice were taken at the same time points on the first day of injection and every other 10- or 15-days afterwards up to 150 days. On the first day of injection (day 0), the mean body weight of PBS- and NA/STZ-injected mice were comparable ( $19.03 \pm 1.25$  g vs  $18.45 \pm 0.65$  g, respectively;  $p = 0.1339$ ).

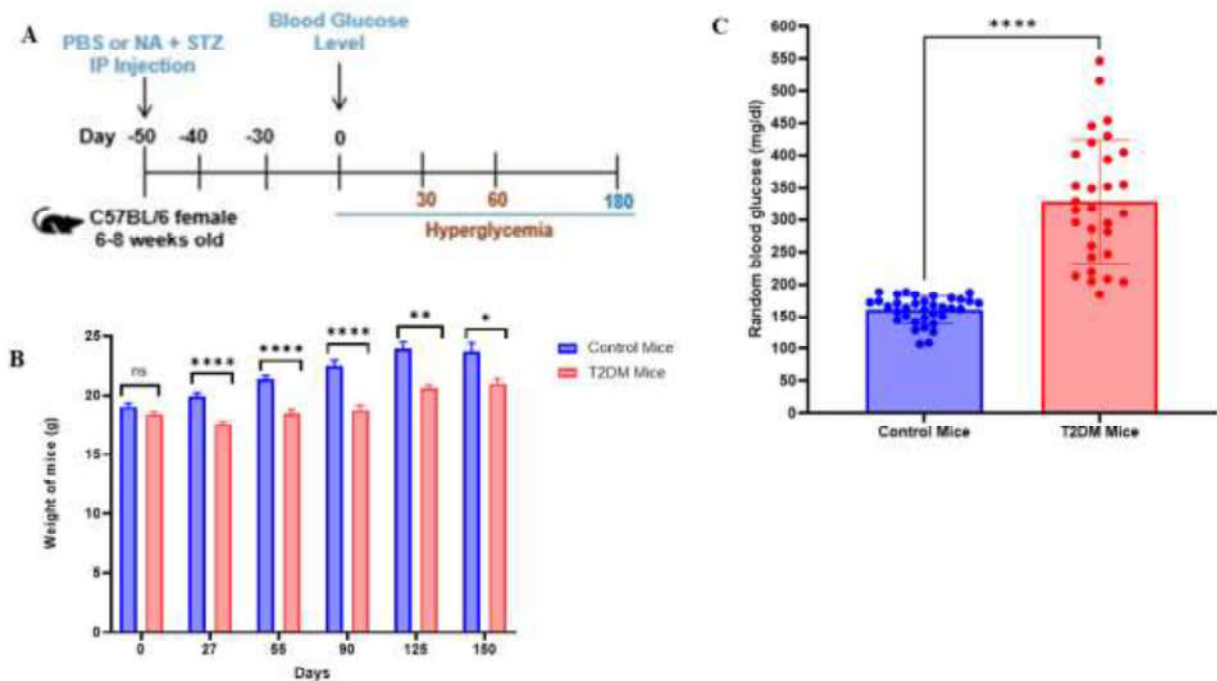


### Figure 1. NA/STZ injection reduces body weight and increases blood glucose levels of C57BL/6 wild-type female mice.

Six- to eight-weeks old pathogen-free C57BL/6 female mice received 60 mg/kg nicotinamide (NA) followed by 180 mg/kg streptozotocin (STZ) 15 minutes after the NA injection. As a control, phosphate-buffered saline (PBS) was given to a second group of mice. NA/STZ and PBS were administered intraperitoneally. Two additional injections of NA/STZ or PBS were given at 10 days interval. **A**. Schematic representation of T2DM induction in C57BL/6 mice. **B**. The body weight of the mice was measured every 10 or 15 days and **C**. Random blood glucose (RBG) levels of the two groups of mice were measured before euthanizing mice for experiments ( $n = 35$  control mice and  $n = 30$  NA/STZ mice). Data analysis and comparison between groups was drawn using paired t-test.  $P < 0.05$  was considered statistically significant. The NA/STZ-injected mice had significantly higher random blood glucose levels but lesser weight compared to PBS-injected mice. The RBG level of five NA/STZ-injected mice were excluded from the data analysis because their values were beyond the range of the instrument. \*\*\*\*,  $p < 0.0001$ ; \*\*,  $p = 0.0025$ ; \*,  $p = 0.036$  between groups.

At 27 days, the average weight of PBS-injected mice was significantly higher than that of the NA/STZ-injected mice ( $19.94 \pm 1.26$  g vs  $17.51 \pm 1.12$  g, respectively;  $p < 0.0001$ ).

Again, at 55 days, the average weight of the PBS-injected mice remained significantly higher than that of NA/STZ-injected mice ( $21.35 \pm 1.41$ g vs  $18.51 \pm 1.30$ g, respectively;  $p < 0.0001$ ), likewise at 90 days ( $22.50 \pm 1.79$ g vs  $18.76 \pm 1.55$ g, respectively;  $p < 0.0001$ ). NA/STZ mice began to gain weight at 125 days, but their average weight was still significantly lower than that of the PBS-injected mice ( $23.90 \pm 1.49$ g vs  $20.60 \pm 0.71$ g, respectively;  $p < 0.0025$ ,  $n = 6$  per group). The average weight of the NA/STZ mice further improved at 150 days, nonetheless it was significantly lower than the average weight of the PBS-injected mice ( $23.68 \pm 1.90$ g vs  $21.00 \pm 0.95$ g, respectively;  $p < 0.036$ ,  $n = 6$  per group). Even though both groups of mice continued to gain weight after four weeks of the first injection, PBS-injected mice gained weight at a faster rate compared to the NA/STZ-injected group (approximately 24.44% vs 13.82% weight gain, respectively, at 150 days). The details are shown in Figure 1B.

#### Blood glucose levels of the mice

One month after the third dose of PBS- and NA/STZ-injections, the mean random blood glucose (RBG) level of the three randomly selected mice from each group were  $143.00 \pm 21.96$  mg/dl and  $336.33 \pm 44.39$  mg/dl respectively. Thereafter, the RBG levels of mice were tested before each experiment. The RBG level of PBS-injected mice ranged from 107.00 mg/dl to 188.00 mg/dl with a mean of  $160.50 \pm 3.60$  mg/dl while that of NA/STZ-injected mice ranged from 185.00 mg/dl to 547.00 mg/dl, respectively, with a mean of  $327.90 \pm 17.48$  mg/dl. Taken together, the NA/STZ-injected mice had significantly higher RBG levels compared to the PBS-injected mice (Figure 1 C;  $p < 0.0001$ ). The RBG level of five NA/STZ-injected mice were excluded from the data analysis because their values were very high and beyond the range of the instrument. Mice

which received PBS injections are hereinafter referred to as control mice and the NA/STZ-injected ones as T2DM mice.

#### Purity of isolated lung macrophages

Lung and peritoneal macrophages were cultured as mentioned previously and purity was checked by flow cytometry as described in the methods section. Two independent experiments were performed, and cell viability was found to be 95.0% to 98.8% (Figure 2A). Out of these cells, 73.1% to 82.8% were leukocytes (CD45+) and of these leukocytes, ninety-five percent of them were lung macrophages (F4/80+ cells). We found alveolar macrophages (CD45+F4/80+Siglec F+) were between 40.4% to 81.4% of the lung macrophages and interstitial macrophages (CD45+F4/80+CD11b+) were between 17.2% to 58.7% of the lung macrophages.

#### Purity of isolated peritoneal macrophages

Three experiments were performed to check the purity of peritoneal macrophages (Figure 2B). Almost all the attached peritoneal cells (99.0% to 99.3%) were live cells (Aqua Live/Dead+) and about two-thirds (60.4% to 77.4%) of them were leukocytes (CD45+). Nearly all the leukocytes (98.8% to 99.2%) expressed CD11b+. Cells were cultured and washed thrice to remove non-adherent cells to improve the purity of the macrophages.

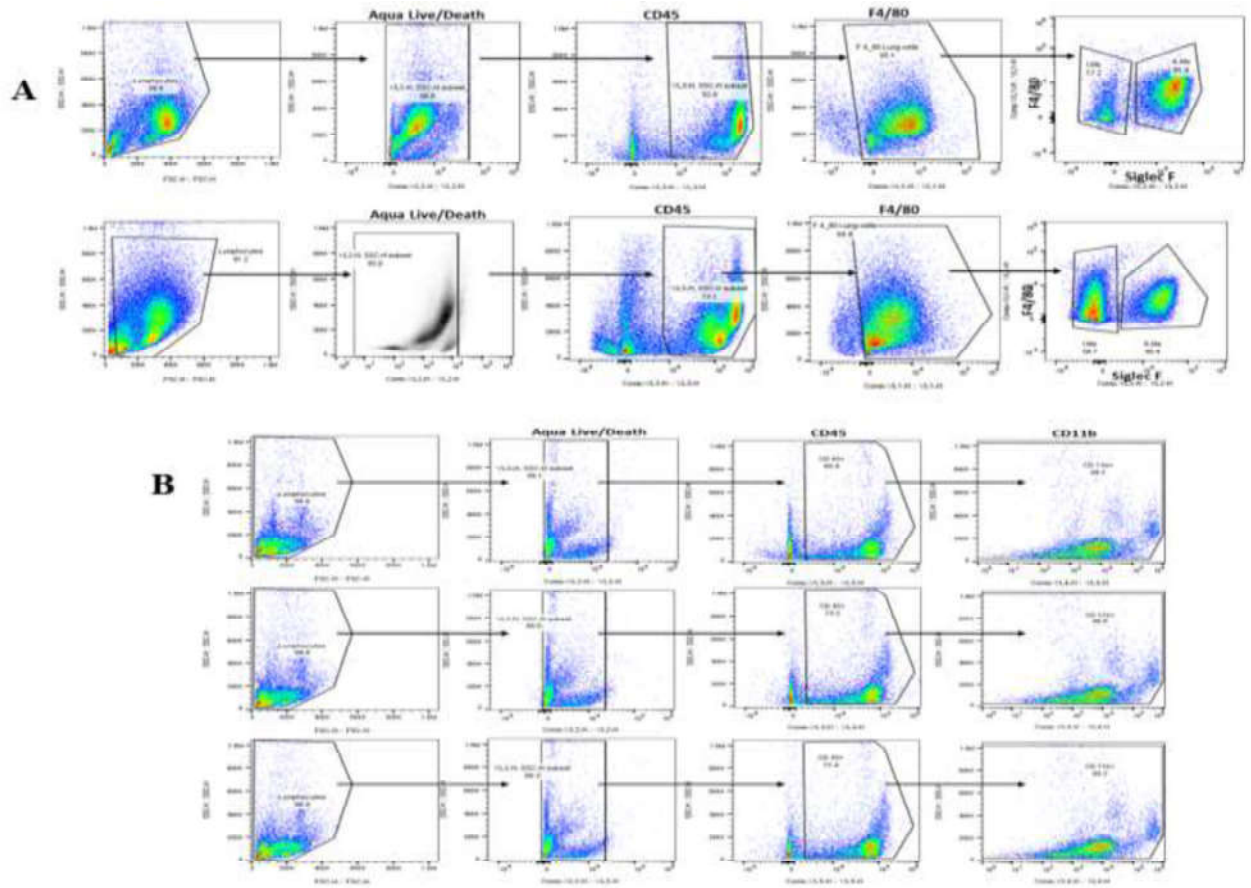


**Figure 3. Representative flow cytometry demonstrating the purity of the isolated alveolar and peritoneal macrophages.**

Total lung and peritoneal macrophages (**A and B, respectively**) were isolated from control C57BL/6 female mice. The cells were cultured for 24 hours in a 5% CO<sub>2</sub> incubator at 37°C. The supernatant was removed, cells were washed twice with 1X HBSS and prepared for flow cytometry. Purity of isolated cells was determined by flow cytometry using Aqua Live/Dead, CD45, F4/80, Siglec F and CD11b. Two experiments were performed to check the purity of lung macrophages (**A**) and three experiments for peritoneal macrophages (**B**).

Recombinant IL-22 had no effect on the viability of lung and peritoneal macrophages

Isolated murine lung and peritoneal macrophages were cultured with or without 10 µg/ml gamma-irradiated *Mtb* ( $\gamma$ -*Mtb*) and in the presence or absence of recombinant IL-22 (10 ng/ml) for

24- and 72-hours, respectively. After 24- and 72-hours cell viability was measured using lactate dehydrogenase (LDH) assay as described in the methods section. As shown in Figure 3, there is no significant difference in the cell viability between control,  $\gamma Mtb$  and  $\gamma Mtb$  + recombinant IL-22 cultured macrophages at the two time points. The maximal LDH activity represents the upper

limits of cytotoxicity when the cells were lysed.

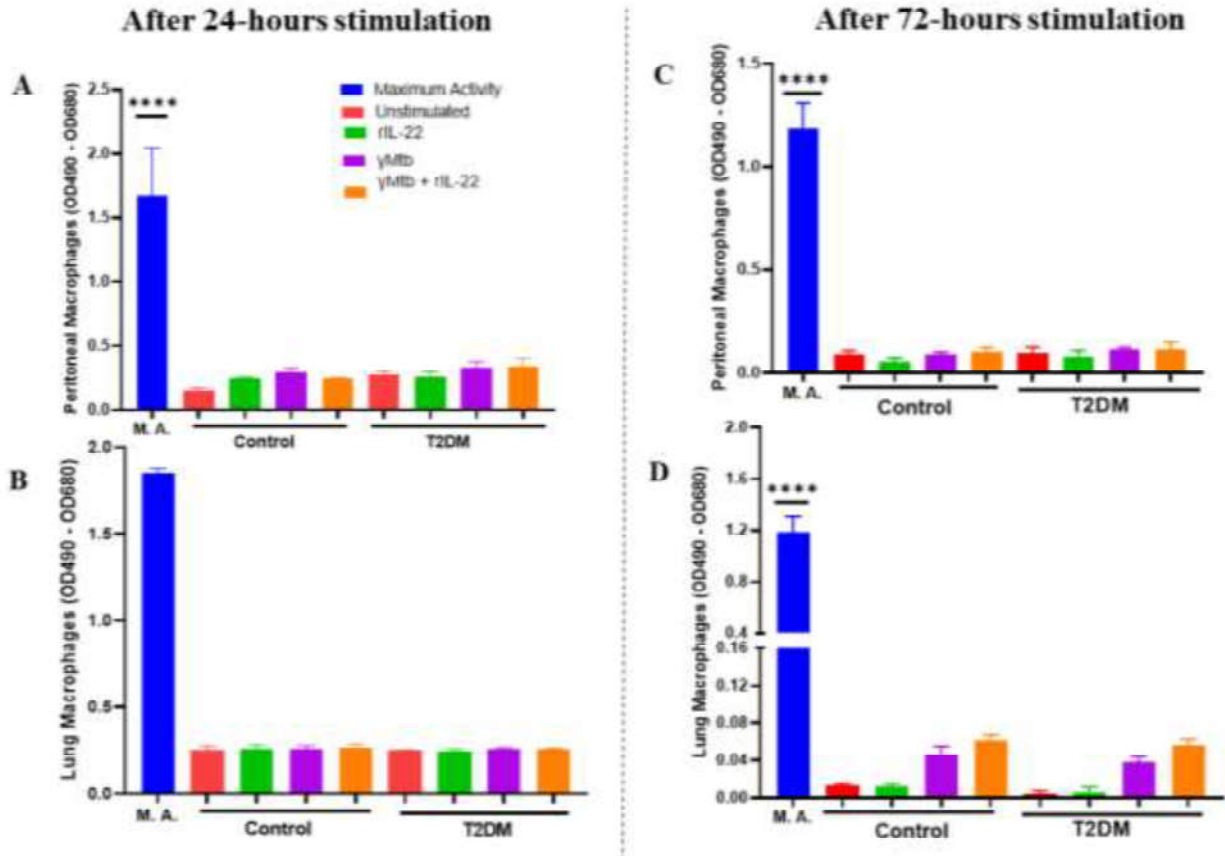


**Figure 5. Recombinant interleukin-22 has no effect on viability of  $\gamma$ Mtb-cultured macrophages.**

Peritoneal and lung macrophages were isolated from control and T2DM C57BL/6 mice and cultured in 24 well plate with or without 10  $\mu$ g/ml  $\gamma$ -Mtb and in the presence or absence of recombinant IL-22 (10 ng/ml) for 24- and 72- hours. After 24 and 72 hours (**A and B; C and D, respectively**) cell viability was measured using lactate dehydrogenase assay as mentioned in methods section. Three independent experiments (n = 3) were performed for panels **A, C-D** and two independent experiments (n = 2) were performed for 24-hours stimulated lung macrophages (**B**). Data was analyzed using GraphPad prism version 9.3.1.471 and comparison between samples was determined by one-way ANOVA followed by Tukey's multiple comparison test. Statistically significant *p-value* was set at < 0.05. \*\*\*\* *p* < 0.0001 for each sample compared to the upper limit of cytotoxicity (maximum activity).



Recombinant IL-22 inhibits the expression of necroptotic marker pMLKL by *Mtb*-cultured T2DM mice lung macrophages

We cultured isolated control and T2DM mice macrophages with  $\gamma$ *Mtb* (10  $\mu$ g/ml) and with or without rIL-22 (10 ng/ml). After 72 hours, expression of necroptotic markers pMLKL and total MLKL of all samples of macrophages were determined by western blot (Figure 4). In three independent experiments,  $\gamma$ *Mtb*-stimulation of T2DM mice lung macrophages significantly increased the expression of pMLKL compared to  $\gamma$ *Mtb* stimulated non-T2DM control mice lung macrophages ( $p = 0.0201$ ). rIL-22 treatment significantly reduced the expression of pMLKL by  $\gamma$ *Mtb*-stimulated lung macrophages of T2DM mice ( $p = 0.00064$ ). The expression of pMLKL levels were normalized with the respective  $\beta$ -actin (Figure 4). The levels of total MLKL were inconsistent in the three experiments, however blot quantification showed that rIL-22 treatment reduced the expression of pMLKL when normalized to that of respective total MLKL in  $\gamma$ *Mtb*-stimulated lung macrophages of T2DM mice (Supplementary Figure 2).

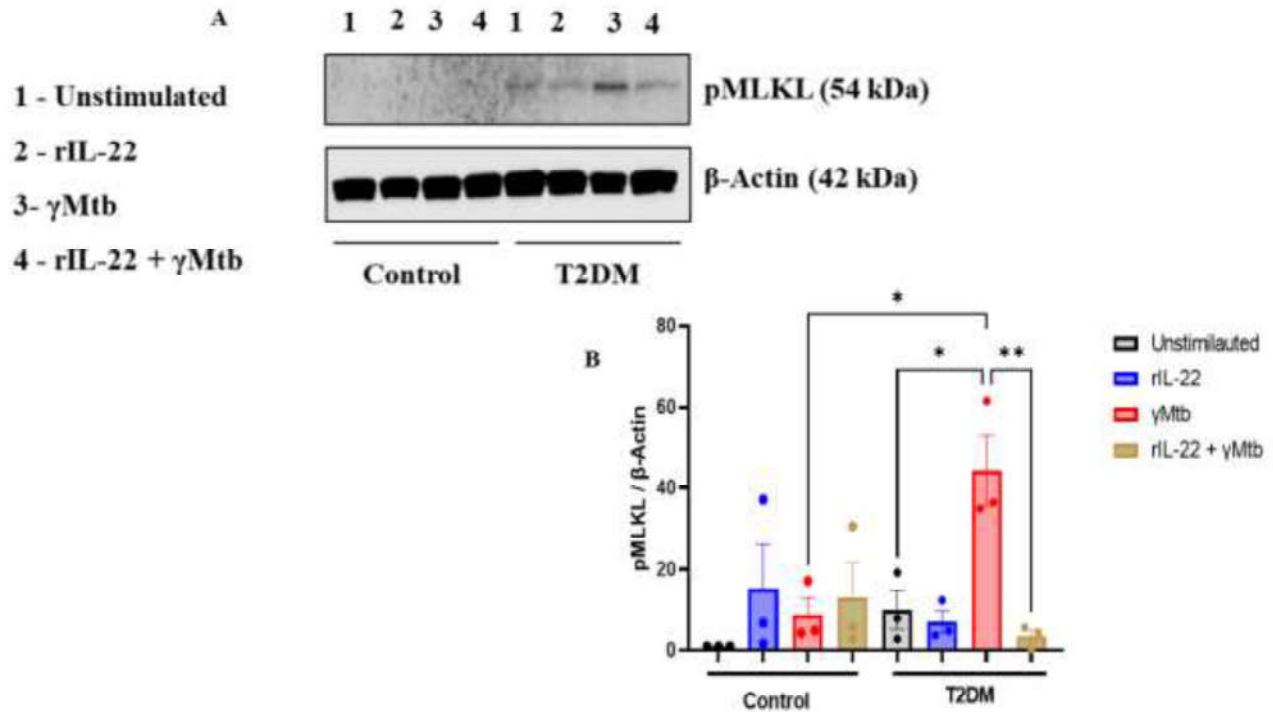


**Figure 7. Recombinant IL-22 reduces expression of pMLKL protein in  $\gamma$ -irradiated Mtb-stimulated mice lung macrophages of T2DM mice.**

Lung macrophages were isolated from control and T2DM C57BL/6 female mice (two groups of age-matched mice). The cells were cultured with or without 10  $\mu$ g/ml  $\gamma$ -Mtb and in the presence or absence of recombinant IL-22 (10 ng/ml) for 72 hours. After 72 hours the supernatants were removed, and the cellular proteins were extracted. Western blot was performed to determine the expression of pMLKL in three independent experiments (n = 3) (A). Protein levels were then normalized with the level of  $\beta$ -actin (B). Pooled cells from three mice per group were used for each experiment. Statistically significant *p*-value was set at < 0.05. \*\* *p* = 0.0064; \* *p* < 0.0259.

Next, we performed one experiment to determine the necroptotic markers using peritoneal macrophages from control and T2DM mice. As shown in Figure 5, we found that rIL-22 reduced the expression of pRIPK3 and pMLKL in T2DM mice macrophages cultured with  $\gamma$ Mtb. Although, additional experiments are needed to confirm these findings.

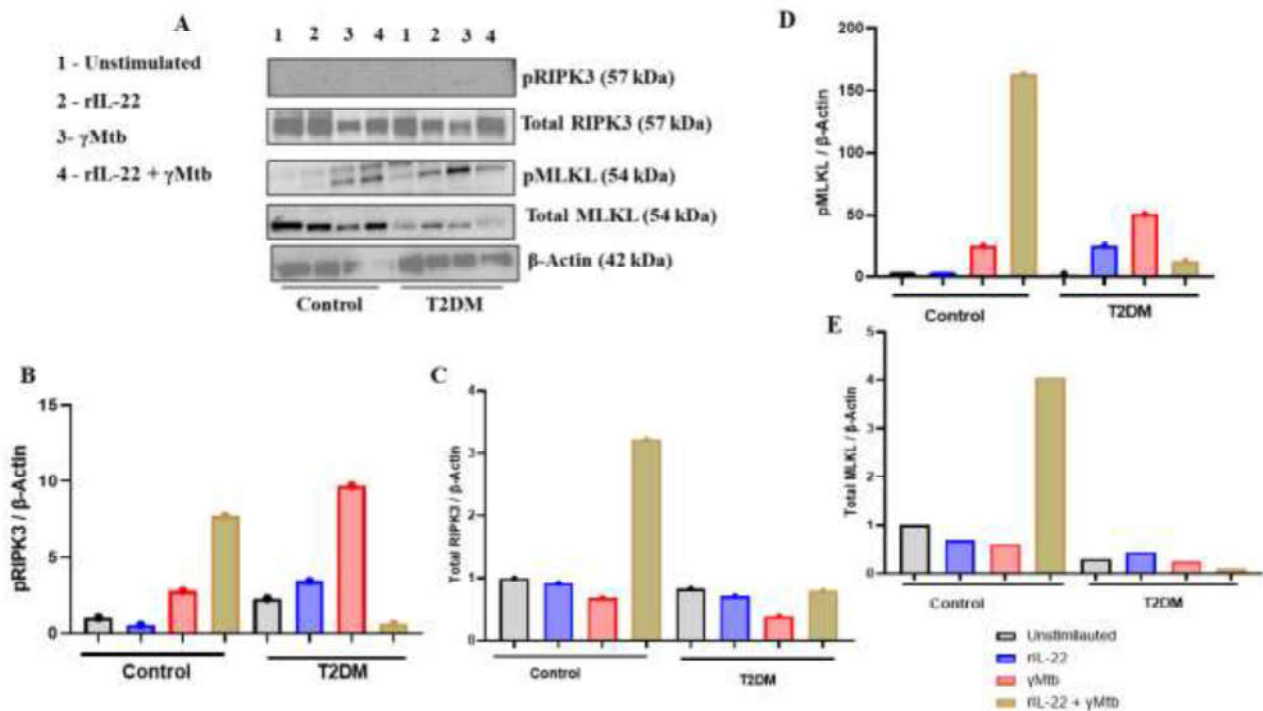


**Figure 9. Recombinant IL-22 reduces expression of pRIPK3 and pMLKL proteins in  $\gamma$ Mtb-stimulated peritoneal macrophages of T2DM mice.**

Peritoneal macrophages were isolated from control and T2DM C57BL/6 female mice (two groups of age-matched mice). Pooled cells from three mice per group were used for this experiment. The cells were cultured with or without 10  $\mu$ g/ml  $\gamma$ -Mtb and in the presence or absence of recombinant IL-22 (10 ng/ml) for 72 hours. After 72 hours the supernatants were removed, and the cellular proteins extracts were prepared. Western blot was performed to determine the expression of total RIPK3, total MLKL, pRIPK3 and pMLKL levels in one experiment (n = 1) (A). Protein levels were then normalized with the level of  $\beta$ -actin (B and E).

Recombinant IL-22 has no effect on TNF-  $\alpha$  and IL-6 production by  $\gamma$ Mtb-cultured T2DM mice macrophages

We cultured isolated control and T2DM mice lung and peritoneal macrophages with  $\gamma$ Mtb (10  $\mu$ g/ml) and rIL-22 (10 ng/ml). After 24 hours, TNF-  $\alpha$  (Figure 6A and C) and IL-6 (Figure 6B and D) levels in the culture supernatants were measured by ELISA. The results from five independent experiments suggest that  $\gamma$ -irradiated *Mtb* significantly increased the production of

IL-6 in both control and diabetic mice peritoneal macrophages ( $p < 0.0001$ ). However, rIL-22 treatment had no effect on TNF- $\alpha$  and IL-6 production by  $\gamma$ Mtb-cultured T2DM mice peritoneal macrophages. Similar findings were observed in two independent experiments performed with lung macrophages.

Further, we repeated these by performing three independent experiments in the culture supernatants of peritoneal and lung macrophages as well as total splenocytes after 72 hours

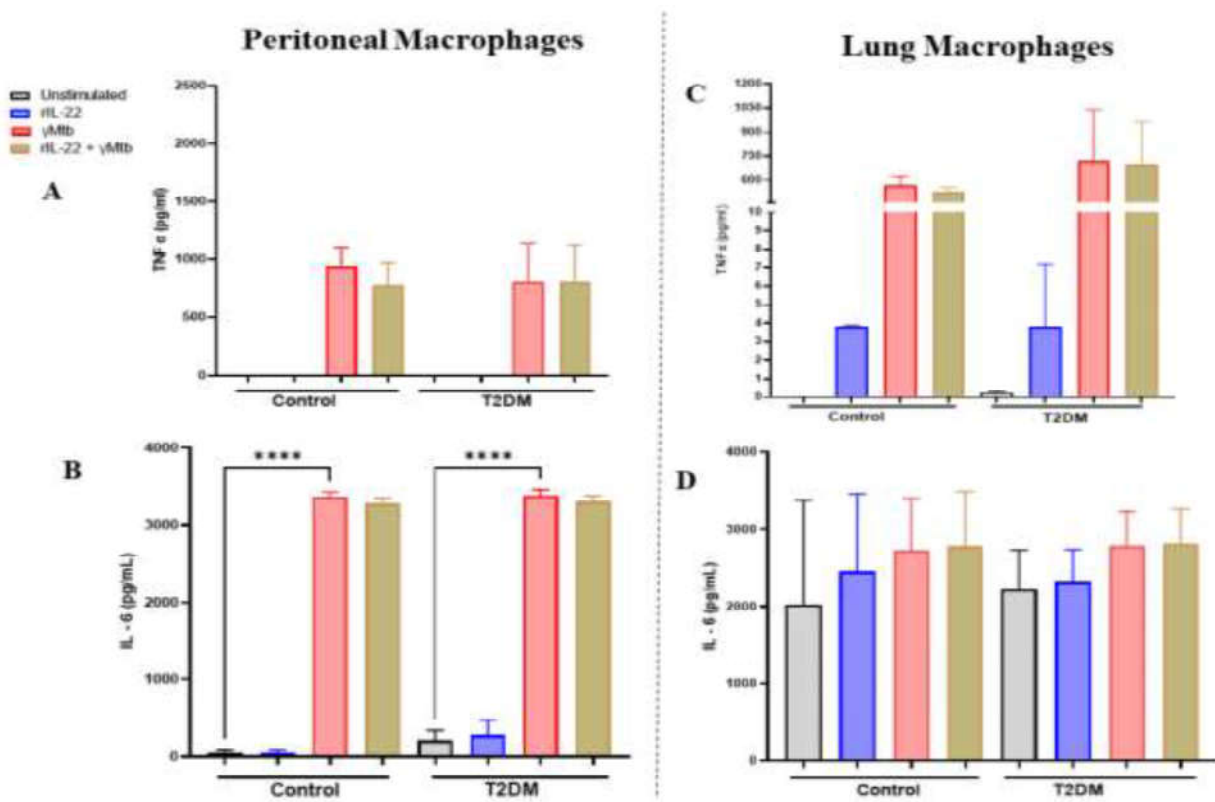


**Figure 11. Recombinant IL-22 has no effect on TNF-  $\alpha$  and IL-6 production by  $\gamma$ Mtb-stimulated macrophages of T2DM mice.**

Peritoneal (A and B) and lung macrophages (C and D) were isolated from control and T2DM C57BL/6 female mice (two groups of age-matched mice) and cultured with or without 10  $\mu$ g/ml  $\gamma$ -Mtb and in the presence or absence of recombinant IL-22 (10 ng/ml) for 24 hours. TNF-  $\alpha$  (A and C) and IL-6 (B and D) levels in the culture supernatants were measured by ELISA. Data is representative of five independent experiments (n = 5) from peritoneal macrophages and two independent experiments (n = 2) from lung macrophages. Cells from 3 mice were pooled per group for each experiment. Statistically significant  $p$ -value was set at  $< 0.05$ . \*\*\*\*  $p < 0.0001$ .

stimulation with and without  $\gamma$ *Mtb* (10  $\mu$ g/ml) and rIL-22 (10 ng/ml). Again, rIL-22 treatment did not alter the TNF- $\alpha$ , IL-6 and interferon gamma (IFN- $\gamma$ ) production by  $\gamma$ *Mtb*-cultured T2DM mice macrophages and splenocytes (Supplementary Figure 1).

AIM 2: Determine whether IL-22 regulates metabolism (glycolysis and oxidative phosphorylation) of *Mtb*-stimulated macrophages from T2DM mice.

Diabetes is a chronic metabolic disorder. Therefore, we determined whether rIL-22 restores the metabolic state of  $\gamma$ *Mtb*-cultured macrophages of T2DM mice. We performed a metabolic flux assay to detect changes in the mitochondrial oxygen consumption rate (OCR) and extracellular acidification rate (ECAR) as measures of oxidative phosphorylation and glycolysis, respectively.

Recombinant IL-22 has no effect on oxidative phosphorylation of  $\gamma$ *Mtb*-cultured T2DM mice peritoneal macrophages

We did not perform mitochondrial-stress assay using lung macrophages due to limited number of mice and lung macrophages. However, we performed this assay using peritoneal macrophages to determine whether recombinant IL-22 affects the oxygen consumption rate (OCR) of  $\gamma$ *Mtb*-cultured peritoneal macrophages from control and T2DM mice (Figure 7). Data from five independent experiments showed that  $\gamma$ *Mtb*-stimulation of peritoneal macrophages in control mice significantly reduced the ATP-linked respiration (Figure 7C,  $p = 0.0073$ ), maximum respiration (Figure 7D,  $p = 0.0052$ ) and spare respiration (Figure 7E,  $p = 0.0028$ ). In addition, ATP-linked respiration was significantly lower in unstimulated T2DM mice peritoneal macrophages compared to unstimulated peritoneal macrophages from control mice (Figure 7C,  $p = 0.0182$ ). Recombinant

IL-22 could not restore these reduced respiratory parameters in control and T2DM mice peritoneal macrophages ( $p > 0.05$ ). Details are shown in Figure 7.

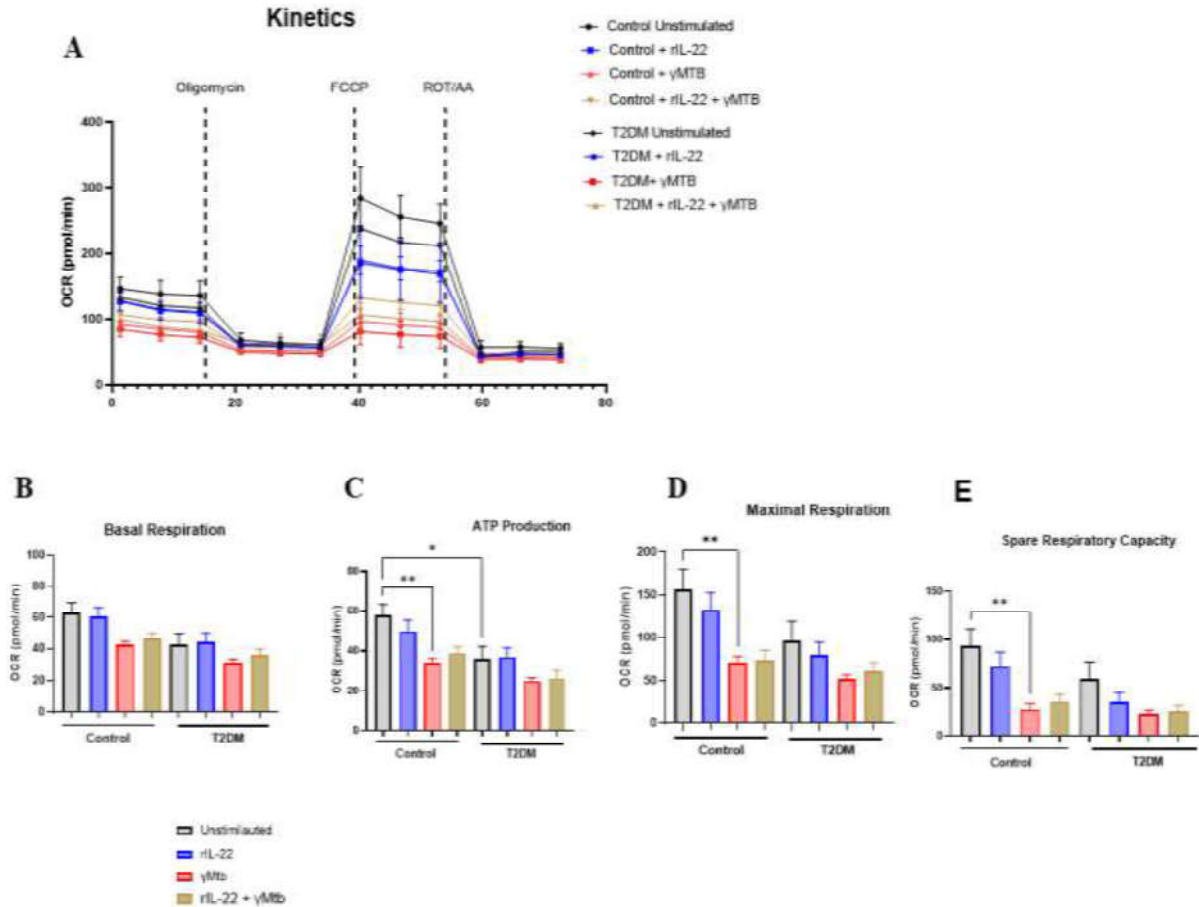


**Figure 13. Recombinant IL-22 has no effect on oxidative phosphorylation of  $\gamma$ Mtb-stimulated peritoneal macrophages of T2DM mice.**

Peritoneal macrophages were isolated from control and T2DM C57BL/6 female mice (two groups of age-matched mice) and cultured with or without 10  $\mu$ g/ml  $\gamma$ Mtb and in the presence or absence of recombinant IL-22 (10 ng/ml) for 48 hours. After 48 hours, the supernatants were removed, and the kinetics of oxidative phosphorylation (A), basal respiration (B), ATP-linked respiration (C), maximal respiration (D) and spare respiratory capacity (E) were determined by Agilent Seahorse XF Cell Mito Stress Test. Each experiment was performed with pooled cells from three mice. Experiments were repeated five times ( $n = 5$ ) and GraphPad prism version 9.3.1.471 was used for data analysis. Comparison between samples was determined by one-way ANOVA followed by Tukey’s multiple comparison test.  $P < 0.05$  was considered statistically significant. \*\*  $p < 0.0075$ ; \*  $p = 0.0182$ .

Recombinant IL-22 has no effect on the extracellular acidification rate of  $\gamma$ Mtb-stimulated peritoneal macrophages from T2DM mice

Gamma-*Mtb* stimulation of T2DM mice peritoneal macrophages resulted in significant elevation of the extracellular acidification rate (ECAR) of the basal glycolysis (Figure 8B,  $p = 0.0081$ ) compared to unstimulated T2DM mice peritoneal macrophages in three independent

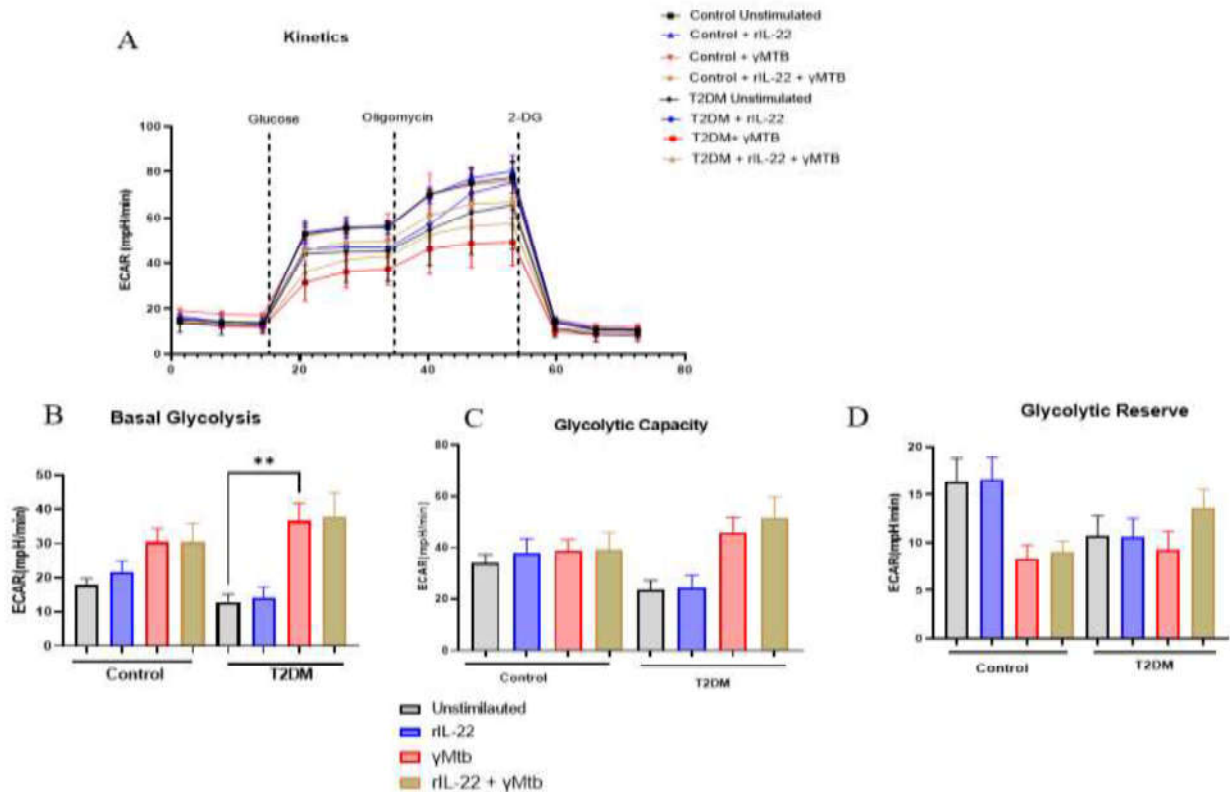


**Figure 15. Recombinant IL-22 has no effect on extracellular acidification rate of  $\gamma$ Mtb-stimulated peritoneal macrophages.**

Peritoneal macrophages were isolated from control and T2DM C57BL/6 female mice (two groups of age-matched mice) and cultured with or without 10  $\mu$ g/ml gamma-irradiated *Mtb* and in the presence or absence of recombinant IL-22 (10 ng/ml) for 48 hours. After 48 hours, the supernatants were removed and kinetics of glycolysis (A), basal glycolysis (B), glycolytic capacity (C) and glycolytic reserve (D) of the pellets was determined by Agilent Seahorse XF Glycolysis Stress Test. Each experiment was performed with pooled cells from three mice. Three independent experiments ( $n = 3$ ) were performed. GraphPad prism version 9.3.1.471 was used for data analysis. Comparison between samples was determined by one-way ANOVA followed by Tukey's multiple comparison test.  $P < 0.05$  was considered statistically significant. \*\*  $p = 0.0081$ .

experiments (Figure 8). rIL-22 treatment of  $\gamma$ Mtb-cultured peritoneal macrophages from T2DM mice did not cause any significant change in the basal glycolysis ( $p > 0.05$ ).

Recombinant IL-22 has no effect on the extracellular acidification rate of  $\gamma$ Mtb-stimulated lung macrophages from T2DM mice

Three independent experiments were performed to determine glycolysis in lung macrophages. The data indicate that basal glycolysis, glycolytic capacity, and glycolytic reserve were marginally reduced in T2DM mice lung macrophages without any stimulation compared to that of control mice (Figure 9B-D, respectively). These values are not statistically significant. However, in T2DM mice,  $\gamma$ Mtb-stimulation of lung macrophages significantly elevated the basal glycolysis (Figure 9B,  $p = 0.0001$ ) and glycolytic capacity (Figure 9C,  $p = 0.0013$ ) compared to the unstimulated macrophages.  $\gamma$ Mtb stimulation marginally increased the basal glycolysis, glycolytic capacity, and glycolytic reserve of T2DM lung macrophages compared to  $\gamma$ Mtb stimulation of control mice lung macrophages, but the values are not statistically significant. Recombinant IL-22 slightly reduced all these levels of glycolytic parameters in  $\gamma$ Mtb-cultured lung macrophages, but the values are not statistically significant (Figure 9).



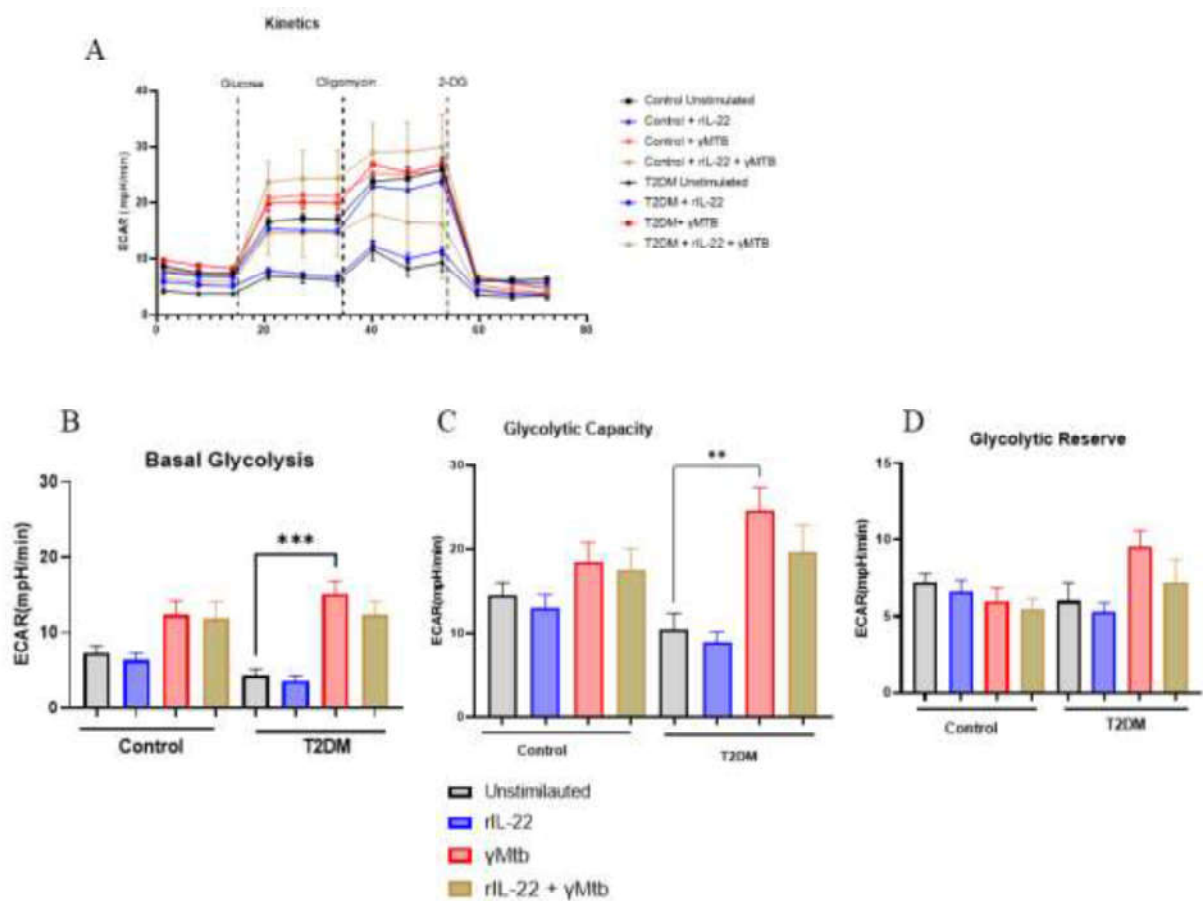


**Figure 17. Recombinant IL-22 has no effect on extracellular acidification rate of  $\gamma$ Mtb-stimulated lung macrophages from T2DM mice.**

Lung macrophages were isolated from control and T2DM C57BL/6 female mice (two groups of age-matched mice) and cultured with or without 10  $\mu$ g/ml  $\gamma$ Mtb and in the presence or absence of recombinant IL-22 (10 ng/ml) for 48 hours. After 48 hours incubation, the supernatants were removed and kinetics of glycolysis (A), basal glycolysis (B), glycolytic capacity (C) and glycolytic reserve (D) of the cells was determined by Agilent Seahorse XF Glycolysis Stress Test. Each experiment was performed with pooled cells from three mice and the experiments were repeated three times (n = 3). GraphPad prism version 9.3.1.471 was used for data analysis. Comparison between samples was determined by one-way ANOVA followed by Tukey's multiple comparison test.  $P < 0.05$  was considered statistically significant. \*\*\*  $p = 0.0001$ . \*\*  $p = 0.0013$ .

## DISCUSSION

T2DM in TB patients worsens the disease and can enhance the mortality [29]. Limited information is available about the immune responses during *Mtb* infection in type 2 diabetic hosts [30]. Our laboratory developed an experimentally induced type 2 diabetes (T2DM) model in wild-type C57BL/6 mice and found that *Mtb* infection in T2DM mice drives pathological immune responses and mortality [11]. IL-22 and type 3 innate lymphoid cells (ILC3s) reduce inflammation and mortality of *Mtb* infected T2DM mice [12]. The laboratory also found that IL-6 enhances inflammatory cytokine production [11] and IL-22 levels were low in pulmonary tuberculosis patients with type 2 diabetes [12]. In unpublished studies, we found that *Mtb*-infected F4/80+CD11c+ alveolar macrophages (AMs) from T2DM mice undergo necroptosis (among 5 death pathways tested) compared to *Mtb*-infected AMs of non-T2DM mice and undergo TNFR1 mediated necroptosis.

In the current study, we tested the hypothesis that recombinant IL-22 treatment inhibits the molecules involved in the necroptotic signaling pathway to reduce inflammatory cytokine production by T2DM mice macrophages stimulated with  $\gamma$ *Mtb*. We also determined whether IL-22 helps to maintain homeostatic glycolysis of  $\gamma$ *Mtb*-stimulated T2DM mice macrophages to reduce necroptosis and inflammation. We found that recombinant IL-22 treatment inhibits the expression of pMLKL (molecule involved in necroptosis) protein by  $\gamma$ *Mtb*-cultured T2DM mice lung macrophages. Recombinant IL-22 treatment had no effect on IL-6 and TNF- $\alpha$  production by T2DM mice macrophages stimulated with  $\gamma$ *Mtb*. We also found recombinant IL-22 has no effect on metabolism (glycolysis and oxidative phosphorylation) of  $\gamma$ *Mtb*-cultured T2DM mice macrophages.

During T2DM, the functional capacity of macrophages and other innate immune cells is significantly compromised [31]. This contributes to increased susceptibility of diabetic patients to *Mtb* and delayed initiation of adaptive immunity [32]. T2DM also can lead to treatment failure in tuberculosis patients [29]. An experimental study indicated that the function of *Mtb*-infected alveolar macrophages is impaired in hyperglycemic mice compared to control mice, resulting in a “reduced expression of signals and chemokines that recruit macrophages” [33]. Thus, the confluence of these two diseases presents a significant threat to global public health and presents an opportunity to further investigate the key immune elements that may be relevant to the treatment of tuberculosis in diabetic patients.

In the current study, we used our well established Streptozotocin (STZ) and nicotinamide (NA) model to induce T2DM in mice. STZ is a broad spectrum antibiotic and diabetogenic agent isolated from *Streptomyces achromogenes* [34], [35]. It selectively destroys pancreatic islet  $\beta$ -cells and several rodents including mice have been found to be sensitive to its cytotoxic effects [19], [36]. The resultant pathology of STZ-induced diabetes mimics human type 1 diabetes [19], however simultaneous administration with nicotinamide (NA) partially protects the pancreatic  $\beta$ -cells against the diabetogenic effect of STZ [37], [38]. Therefore, the two compounds were concurrently administered to induce T2DM in the mice. We found STZ and NA combination induces T2DM in mice confirming our previous study [11].

We followed control and T2DM mice up to 150 days and measured the body weights. The body weights of the diabetic mice increased, but it was significantly lower compared to that of the control mice (Figure 1B). We found that, random blood glucose (RBG) levels of the diabetic mice were significantly higher than that of the control mice (Figure 1C). Our results demonstrates that

induction of T2DM using STZ/NA reduces body weight of mice confirming our previous findings [39].

IL-22 is expressed by cells of both the innate and adaptive immune system such as CD4 T cells (especially T<sub>h</sub>17 cells, and  $\gamma\delta$  T cells), NK cells, LTi cells and LTi-like cells [40]. It is well documented that exogenous IL-22 and the IL-22 receptor pathway promote the migration and survival of cells [41]–[44] and increases the survival of experimental animals [45], [46]. We found that rIL-22 is not cytotoxic to both control and T2DM murine peritoneal and lung macrophages cultured with  $\gamma$ -irradiated *Mtb* (Figure 3).

Unpublished studies from our laboratory demonstrated that AMs from *Mtb*-infected T2DM mice are more necroptotic compared to *Mtb*-infected AMs from non-T2DM mice and that rIL-22 reduces mortality of T2DM mice [12]. We investigated the effect of rIL-22 on the expression and phosphorylation of the necroptotic protein MLKL. In the current study,  $\gamma$ *Mtb*-stimulation significantly increased the expression of pMLKL in T2DM mice lung macrophages confirming our laboratory findings (unpublished) even though  $\gamma$ *Mtb*-stimulation had no effect on cell viability (Figures 3-5). Our findings are in tune with that of Nishihara et al., who posited that  $\gamma$ *Mtb* is able to metabolize but cannot cause infection in susceptible animals [47]. Recombinant IL-22 significantly reduced phosphorylation of MLKL of  $\gamma$ *Mtb*-stimulated T2DM mice lung macrophages. Necroptotic cell death occurs when the activation loop in the executioner protein, MLKL, is phosphorylated [48]–[50]. pMLKL causes plasma membrane rupture by binding to phosphoinositides [51]. Necroptosis between neighboring cells is enhanced by the accumulation of pMLKL at intercellular junctions [49]. Our study for the first time demonstrates that rIL-22 treatment reduces the expression of pMLKL in T2DM mice lung macrophages stimulated with

$\gamma$ *Mtb* (Figure 5). Our findings suggest that rIL-22 could be exploited as a novel therapeutic or prophylactic compound for the treatment of diabetes-tuberculosis co-infection.

Diabetes and diabetes-tuberculosis co-morbidity lead to increased production of the inflammatory cytokines TNF- $\alpha$ , IL-6 and IFN- $\gamma$ , increases the severity of disease and drives mortality [11], [52], [53]. Six months after *Mtb* infection (chronic infection) significant increases in inflammatory cytokines TNF- $\alpha$ , IL-6 and IFN- $\gamma$  in T2DM mice compared to non-diabetic mice infected with *Mtb* were found [11]. In contrast, one month after *Mtb* infection (acute stages) [11] there is no change in inflammatory cytokine levels in *Mtb* infected T2DM mice compared to *Mtb* non-diabetic mice [11]. We found that  $\gamma$ *Mtb*-stimulation of macrophages and splenocytes of control and T2DM mice increased the levels of TNF- $\alpha$  and IL-6 (Fig. 6 and supplementary Fig. 1). But there is no difference in TNF- $\alpha$  and IL-6 production between control and T2DM mice macrophages stimulated with  $\gamma$ *Mtb*. In the current study, we used macrophages from mice two months after the induction of diabetes. The current findings are consistent with our previously published studies that during the early stages of T2DM, *Mtb* infection has no significant effect on development of inflammatory responses [11].

*Mtb*-infection in human macrophages reduces glycolytic parameters and oxygen consumption rate in mitochondria [54] suggesting *Mtb* alters the metabolic threshold of macrophages to adapt to the altered host environment [55], [56]. We found that *Mtb*-stimulation of peritoneal macrophages from non-diabetic and diabetic mice led to reduction of the maximum respiration, ATP-linked respiration and spare respiration (Figure 7) but an increase in glycolytic parameters (Figures 8 and 9). Our findings demonstrates that *Mtb* infected macrophages functionality depends upon ATP production via glycolysis and not oxidative phosphorylation. It

is reported that altered glucose metabolism can directly mediate impaired phagocytosis and antibacterial function [10].

IL-22 treatment maintains glucose homeostasis in *Mtb*-infected T2DM mice [12]. In the current study, rIL-22 had no significant effect on oxygen consumption rates and extracellular acidification rates of  $\gamma$ *Mtb* stimulated T2DM mice macrophages and  $\gamma$ *Mtb* stimulated non-diabetic mice macrophages (Figures 7-9).

In summary, we found  $\gamma$ *Mtb* stimulation of diabetic mice lung and peritoneal macrophages significantly enhanced the expression of pMLKL compared to  $\gamma$ *Mtb* stimulated non-diabetic mice lung and peritoneal macrophages. Recombinant IL-22 significantly inhibited the expression of pMLKL by  $\gamma$ *Mtb* stimulation of mice lung and peritoneal macrophages. In future studies, we will use live *Mtb* strains to infect macrophages and study the effects of rIL-22 on inflammatory responses, necroptosis, and cell metabolism. Further understanding of the mechanisms involved in IL-22 mediated inhibition of pMLKL expression will help to develop therapies to prevent excess inflammation in T2DM individuals with active and latent tuberculosis infection.

## REFERENCES

- [1] R. Singh, S. P. Dwivedi, U. S. Gaharwar, R. Meena, P. Rajamani, and T. Prasad, “Recent updates on drug resistance in *Mycobacterium tuberculosis*,” *J. Appl. Microbiol.*, vol. 128, no. 6, pp. 1547–1567, Jun. 2020, doi: 10.1111/JAM.14478.
- [2] C. R. Stevenson *et al.*, “Diabetes and tuberculosis: The impact of the diabetes epidemic on tuberculosis incidence,” *BMC Public Health*, vol. 7, pp. 1–8, 2007, doi: 10.1186/1471-2458-7-234.
- [3] H. D. Sathkumara *et al.*, “Mucosal delivery of ESX-1–expressing BCG strains provides superior immunity against tuberculosis in murine type 2 diabetes,” *Proc. Natl. Acad. Sci. U. S. A.*, vol. 117, no. 34, pp. 20848–20859, 2020, doi: 10.1073/pnas.2003235117.
- [4] A. Cohen, V. D. Mathiasen, T. Schön, and C. Wejse, “The global prevalence of latent tuberculosis: A systematic review and meta-analysis,” *Eur. Respir. J.*, vol. 54, no. 3, Sep. 2019, doi: 10.1183/13993003.00655-2019.
- [5] R. H. Al-Rifai, F. Pearson, J. A. Critchley, and L. J. Abu-Raddad, “Association between diabetes mellitus and active tuberculosis: A systematic review and meta-analysis,” *PLoS One*, vol. 12, no. 11, pp. 1–26, 2017, doi: 10.1371/journal.pone.0187967.
- [6] J. Cadena, S. Rathinavelu, J. C. Lopez-Alvarenga, and B. I. Restrepo, “The re-emerging association between tuberculosis and diabetes: Lessons from past centuries,” *Tuberculosis (Edinb)*, vol. 116S, pp. S89–S97, May 2019, doi: 10.1016/J.TUBE.2019.04.015.
- [7] M. R. Lee *et al.*, “Diabetes Mellitus and Latent Tuberculosis Infection: A Systematic Review and Metaanalysis,” *Clin. Infect. Dis.*, vol. 64, no. 6, pp. 719–727, Mar. 2017, doi: 10.1093/CID/CIW836.

- [8] World Health Organization, "Global Report on Diabetes," *WHO Press*, vol. 978, p. 88, 2016, doi: ISBN 978 92 4 156525 7.
- [9] B. Ayelign, M. Negash, M. Genetu, T. Wondmagegn, and T. Shibabaw, "Immunological Impacts of Diabetes on the Susceptibility of Mycobacterium tuberculosis," *J. Immunol. Res.*, vol. 2019, 2019, doi: 10.1155/2019/6196532.
- [10] K. Hodgson, J. Morris, T. Bridson, B. Govan, C. Rush, and N. Ketheesan, "Immunological mechanisms contributing to the double burden of diabetes and intracellular bacterial infections," *Immunology*, vol. 144, no. 2, p. 171, Feb. 2015, doi: 10.1111/IMM.12394.
- [11] S. S. Cheekatla *et al.*, "NK-CD11c+ Cell Crosstalk in Diabetes Enhances IL-6-Mediated Inflammation during Mycobacterium tuberculosis Infection," *PLoS Pathog.*, vol. 12, no. 10, Oct. 2016, doi: 10.1371/JOURNAL.PPAT.1005972.
- [12] D. Tripathi *et al.*, "IL-22 produced by type 3 innate lymphoid cells (ILC3s) reduces the mortality of type 2 diabetes mellitus (T2DM) mice infected with Mycobacterium tuberculosis," *PLoS Pathog.*, vol. 15, no. 12, 2019, doi: 10.1371/JOURNAL.PPAT.1008140.
- [13] J. A. Dudakov, A. M. Hanash, and M. R. M. Van Den Brink, "Interleukin-22: immunobiology and pathology," *Annu. Rev. Immunol.*, vol. 33, p. 747, Mar. 2015, doi: 10.1146/ANNUREV-IMMUNOL-032414-112123.
- [14] R. Dhiman, S. Venkatasubramanian, P. Paidipally, P. F. Barnes, A. Tvinnereim, and R. Vankayalapati, "Interleukin 22 Inhibits Intracellular Growth of Mycobacterium tuberculosis by Enhancing Calgranulin A Expression," *J. Infect. Dis.*, vol. 209, no. 4, p.



- 578, Feb. 2014, doi: 10.1093/INFDIS/JIT495.
- [15] R. Dhiman *et al.*, “IL-22 Produced by Human NK Cells Inhibits Growth of Mycobacterium tuberculosis by Enhancing Phagolysosomal Fusion,” *J. Immunol.*, vol. 183, no. 10, pp. 6639–6645, Nov. 2009, doi: 10.4049/JIMMUNOL.0902587.
- [16] K. Ronacher, R. Sinha, and M. Cestari, “IL-22: An Underestimated Player in Natural Resistance to Tuberculosis?,” *Front. Immunol.*, vol. 9, no. SEP, p. 2209, Sep. 2018, doi: 10.3389/FIMMU.2018.02209.
- [17] X. Wang *et al.*, “Interleukin-22 alleviates metabolic disorders and restores mucosal immunity in diabetes,” *Nat. 2014 5147521*, vol. 514, no. 7521, pp. 237–241, Aug. 2014, doi: 10.1038/nature13564.
- [18] S. Z. Hasnain *et al.*, “Glycemic control in diabetes is restored by therapeutic manipulation of cytokines that regulate beta cell stress,” *Nat. Med. 2014 2012*, vol. 20, no. 12, pp. 1417–1426, Nov. 2014, doi: 10.1038/nm.3705.
- [19] B. L. Furman, “Streptozotocin-Induced Diabetic Models in Mice and Rats,” *Curr. Protoc.*, vol. 1, no. 4, p. e78, Apr. 2021, doi: 10.1002/CPZ1.78.
- [20] Miltenyi Biotec, “UltraPure mouse,” *User Guid.*, pp. 1–3.
- [21] ThermoFisher Scientific, “CyQUANT™ LDH Cytotoxicity Assay,” *Prod. Inf. Sheet*, p. 1, 2021, [Online]. Available: <https://www.thermofisher.com/order/catalog/product/C20300>.
- [22] Thermo Scientific, “BCA Protein Assay Kit 23225,” *User Guid.*, no. 2161296, pp. 0–3, 2020.
- [23] I. Santa Cruz Biotechnology, “Western (Immuno-) Blotting,” *User Guid.*, pp. 3800–3802, 2000.

- [24] Cell Signaling Technology, “Western Blotting,” *Elsevier*, vol. 26, no. 1, pp. 3–7, 2018, [Online]. Available: <https://www.sciencedirect.com/science/article/pii/S1046202306000065>.
- [25] BioLegend®, “Mouse TNF- $\alpha$  ELISA MAX Deluxe Set,” *User Guid.*, no. 423501, pp. 7–8.
- [26] BioLegend®, “Mouse IL-6ELISA MAX Deluxe Set,” *User Guid.*, no. 423501, pp. 5–6.
- [27] Agilent Technologies, “Seahorse XF Glycolysis Stress Test Kit User Guide □ Kit 103020-100 WARNING,” *User Guid.*, 2019.
- [28] Agilent Technologies, “Seahorse XF Cell Mito Stress Test Kit User Guide □ Kit 103015-100,” *User Guid.*, 2019.
- [29] N. H. Khalil and R. A. Ramadan, “Study of risk factors for pulmonary tuberculosis among diabetes mellitus patients,” *Egypt. J. Chest Dis. Tuberc.*, vol. 65, no. 4, pp. 817–823, Oct. 2016, doi: 10.1016/J.EJCDT.2016.05.009.
- [30] B. I. Restrepo and L. S. Schlesinger, “Host-pathogen interactions in tuberculosis patients with type 2 diabetes mellitus,” *Tuberculosis (Edinb.)*, vol. 93, no. 0, p. S10, Dec. 2013, doi: 10.1016/S1472-9792(13)70004-0.
- [31] N. Chumburidze-Areshidze, T. Kezeli, Z. Avaliani, M. Mirziashvili, T. Avaliani, and N. Gongadze, “The relationship between type-2 diabetes and tuberculosis,” *Georgian Med. News*, no. 300, pp. 69–74, Mar. 2020.
- [32] T. Vallerskog, G. W. Martens, and H. Kornfeld, “Diabetic Mice Display a Delayed Adaptive Immune Response to Mycobacterium tuberculosis,” *J. Immunol.*, vol. 184, no. 11, pp. 6275–6282, 2010, doi: 10.4049/jimmunol.1000304.

- [33] N. Martinez, N. Ketheesan, K. West, T. Vallerskog, and H. Kornfeld, “Impaired Recognition of Mycobacterium tuberculosis by Alveolar Macrophages From Diabetic Mice,” *J. Infect. Dis.*, vol. 214, no. 11, pp. 1629–1637, Dec. 2016, doi: 10.1093/INFDIS/JIW436.
- [34] N. M. Rakieten, M. L. Rakieten, “Studies on the diabetogenic action of streptozotocin (NSC-37917),” *Cancer Chemother Rep*, vol. 29, pp. 91–8, 1963, Accessed: Mar. 27, 2023. [Online]. Available: <https://pubmed.ncbi.nlm.nih.gov/13990586/>.
- [35] Z. Z. Chaudhry *et al.*, “Streptozotocin is equally diabetogenic whether administered to fed or fasted mice,” *Lab. Anim.*, vol. 47, no. 4, p. 257, Oct. 2013, doi: 10.1177/0023677213489548.
- [36] M. Lazar, P. Golden, M. Furman, and T. W. Lieberman, “Resistance of the rabbit to streptozotocin,” *Lancet*, vol. 292, no. 7574, p. 919, Oct. 1968, doi: 10.1016/S0140-6736(68)91094-5.
- [37] P. Masiello *et al.*, “Experimental NIDDM: Development of a new model in adult rats administered streptozotocin and nicotinamide,” *Diabetes*, vol. 47, no. 2, pp. 224–229, 1998, doi: 10.2337/diab.47.2.224.
- [38] N. Kaur, “Role of Nicotinamide in Streptozotocin Induced Diabetes in Animal Models,” *J. Endocrinol. Thyroid Res.*, vol. 2, no. 1, pp. 1–4, 2017, doi: 10.19080/jetr.2017.02.555577.
- [39] R. K. Radhakrishnan *et al.*, “BCG vaccination reduces the mortality of Mycobacterium tuberculosis–infected type 2 diabetes mellitus mice,” *JCI Insight*, vol. 5, no. 5, 2020, doi: 10.1172/JCI.INSIGHT.133788DS1.
- [40] L. A. Zenewicz and R. A. Flavell, “Recent advances in IL-22 biology,” *Int. Immunol.*, vol.

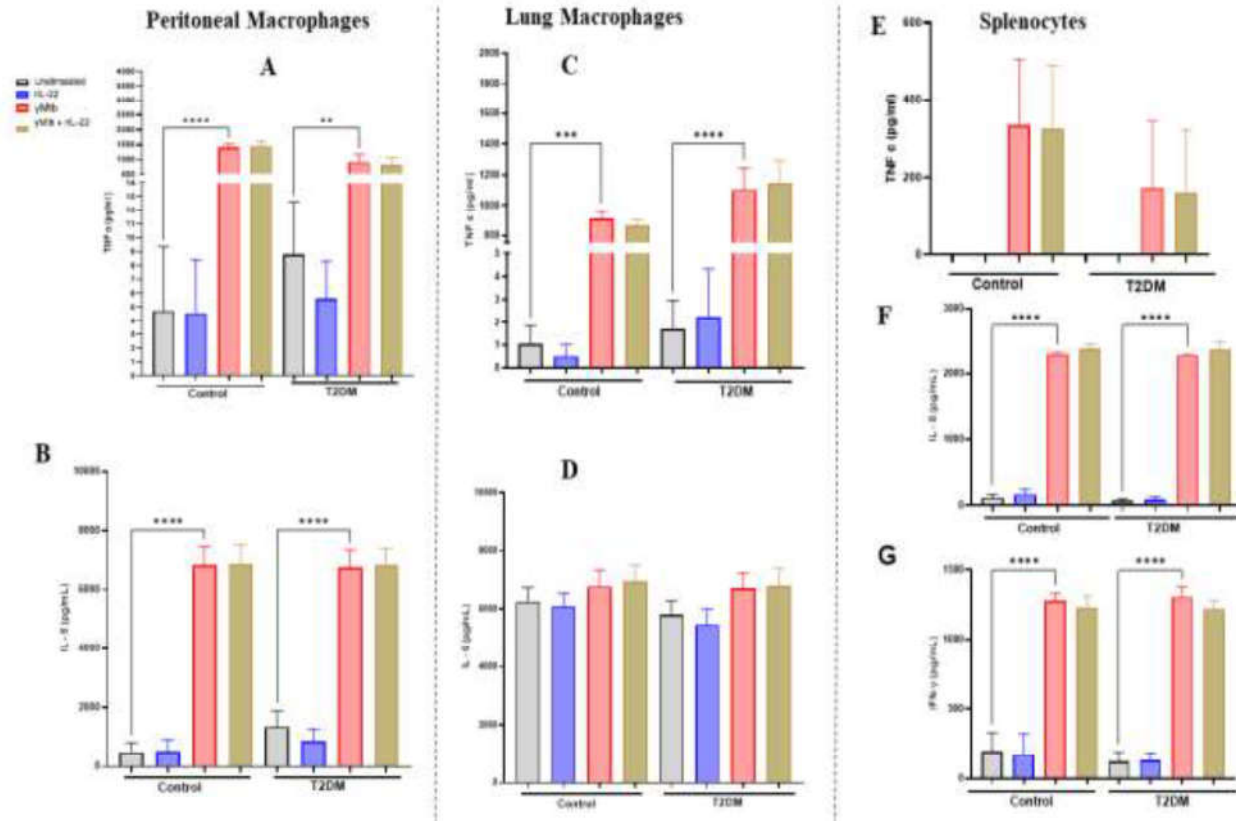
- 23, no. 3, pp. 159–163, Mar. 2011, doi: 10.1093/INTIMM/DXR001.
- [41] H. Akil *et al.*, “IL22/IL-22R Pathway Induces Cell Survival in Human Glioblastoma Cells,” *PLoS One*, vol. 10, no. 3, p. e0119872, Mar. 2015, doi: 10.1371/JOURNAL.PONE.0119872.
- [42] S. Komine-Aizawa, S. Aizawa, C. Takano, and S. Hayakawa, “Interleukin-22 promotes the migration and invasion of oral squamous cell carcinoma cells,” <https://doi-org.abc.cardiff.ac.uk/10.1080/25785826.2020.1775060>, vol. 43, no. 3, pp. 121–129, Jul. 2020, doi: 10.1080/25785826.2020.1775060.
- [43] S. Radaeva, R. Sun, H. N. Pan, F. Hong, and B. Gao, “Interleukin 22 (IL-22) plays a protective role in T cell-mediated murine hepatitis: IL-22 is a survival factor for hepatocytes via STAT3 activation,” *Hepatology*, vol. 39, no. 5, pp. 1332–1342, May 2004, doi: 10.1002/HEP.20184.
- [44] M. E. Keir, T. Yi, T. T. Lu, and N. Ghilardi, “The role of IL-22 in intestinal health and disease,” *J. Exp. Med.*, vol. 217, no. 3, Mar. 2020, doi: 10.1084/JEM.20192195.
- [45] X. Zhang *et al.*, “Second-generation Probiotics Producing IL-22 Increase Survival of Mice After Total Body Irradiation,” *In Vivo (Brooklyn)*, vol. 34, no. 1, pp. 39–50, Jan. 2020, doi: 10.21873/INVIVO.11743.
- [46] D. Tripathi *et al.*, “IL-22 produced by type 3 innate lymphoid cells (ILC3s) reduces the mortality of type 2 diabetes mellitus (T2DM) mice infected with *Mycobacterium tuberculosis*,” *PLoS Pathog.*, vol. 15, no. 12, 2019, doi: 10.1371/JOURNAL.PPAT.1008140.
- [47] H. Nishihara, C. A. Lawrence, G. Taplin, and C. Carpenter, “Immunogenicity of gamma-

- irradiated *Mycobacterium tuberculosis* H37RV (GIV) in mice.,” *Am. Rev. Respir. Dis.*, 1963, doi: 10.1164/ARRD.1963.88.6.827.
- [48] J. M. Hildebrand *et al.*, “Activation of the pseudokinase MLKL unleashes the four-helix bundle domain to induce membrane localization and necroptotic cell death,” *Proc. Natl. Acad. Sci. U. S. A.*, vol. 111, no. 42, pp. 15072–15077, Oct. 2014, doi: 10.1073/PNAS.1408987111/-/DCSUPPLEMENTAL.
- [49] A. L. Samson *et al.*, “MLKL trafficking and accumulation at the plasma membrane control the kinetics and threshold for necroptosis,” *Nat. Commun. 2020 111*, vol. 11, no. 1, pp. 1–17, Jun. 2020, doi: 10.1038/S41467-020-16887-1.
- [50] L. Li, A. Tong, Q. Zhang, Y. Wei, and X. Wei, “The molecular mechanisms of MLKL-dependent and MLKL-independent necrosis,” *J. Mol. Cell Biol.*, vol. 13, no. 1, pp. 3–14, Apr. 2021, doi: 10.1093/JMCB/MJAA055.
- [51] A. Linkermann, U. Kunzendorf, and S. Krautwald, “Phosphorylated MLKL causes plasma membrane rupture,” *Mol. Cell. Oncol.*, vol. 1, no. 1, Jan. 2014, doi: 10.4161/MCO.29915.
- [52] N. P. Kumar, K. Moideen, P. J. George, C. Dolla, P. Kumaran, and S. Babu, “Coincident diabetes mellitus modulates Th1-, Th2-, and Th17-cell responses in latent tuberculosis in an IL-10- and TGF- $\beta$ -dependent manner,” *Eur. J. Immunol.*, vol. 46, no. 2, pp. 390–399, Feb. 2016, doi: 10.1002/EJI.201545973.
- [53] R. S. Eshaq and N. Harris, “The Role of the Inflammatory Mediators TNF- $\alpha$  and IFN- $\gamma$  in the Hyperglycemia-induced PECAM-1 Ubiquitination and Degradation in Diabetic Retinopathy,” *FASEB J.*, vol. 33, no. S1, pp. 685.9-685.9, Apr. 2019, doi: 10.1096/FASEBJ.2019.33.1\_SUPPLEMENT.685.9.

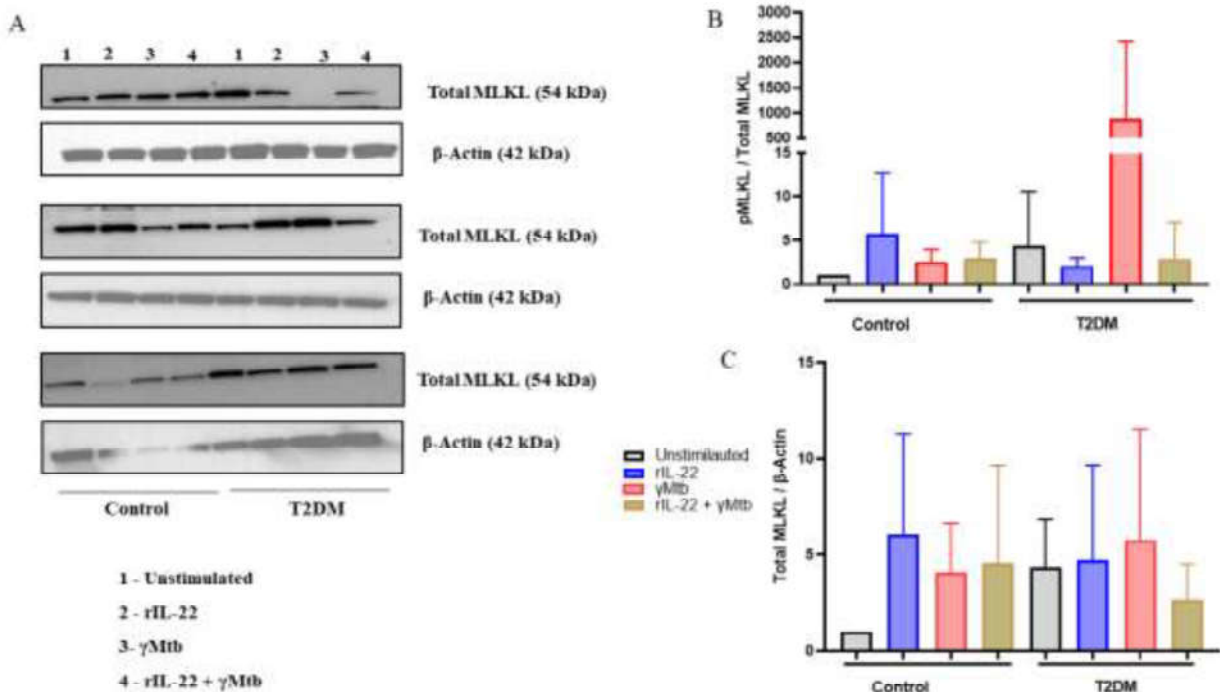
- [54] B. M. Cumming, K. W. Addicott, J. H. Adamson, and A. J. C. Steyn, “Mycobacterium tuberculosis induces decelerated bioenergetic metabolism in human macrophages,” *Elife*, vol. 7, Nov. 2018, doi: 10.7554/ELIFE.39169.
- [55] P. Mehrotra *et al.*, “Pathogenicity of Mycobacterium tuberculosis Is Expressed by Regulating Metabolic Thresholds of the Host Macrophage,” *PLOS Pathog.*, vol. 10, no. 7, p. e1004265, 2014, doi: 10.1371/JOURNAL.PPAT.1004265.
- [56] L. E. Gleeson *et al.*, “Cutting Edge: Mycobacterium tuberculosis Induces Aerobic Glycolysis in Human Alveolar Macrophages That Is Required for Control of Intracellular Bacillary Replication,” *J. Immunol.*, vol. 196, no. 6, pp. 2444–2449, Mar. 2016, doi: 10.4049/JIMMUNOL.1501612.

APPENDIX

Supplementary Materials



**Supplementary Figure 1: Recombinant IL-22 has no effect on TNF- $\alpha$ , IL-6 and IFN- $\gamma$  production by  $\gamma$ Mtb-stimulated macrophages of T2DM mice.** Peritoneal macrophages (A and B), lung macrophages (C and D) and splenocytes (E-G) were isolated from control and T2DM C57BL/6 female mice (two groups of age-matched mice) and cultured with or without 10  $\mu$ g/ml  $\gamma$ -Mtb and in the presence or absence of recombinant IL-22 (10 ng/ml) for 72 hours. TNF- $\alpha$  (A, C and E), IL-6 (B, D and F) and IFN- $\gamma$  (G) levels in the culture supernatants were measured by ELISA. Data is representative of three independent experiments (n = 3) from peritoneal macrophages. Three mice cells were pooled per group for each experiment of peritoneal and lung macrophages. Statistically significant *p*-value was set at < 0.05\*\*\*\*, *p* < 0.0001; \*\*\*, *p* < 0.0009; \*\*, *p* = 0.0012; \*, *p* = 0.0103.



**Supplementary Figure 2: Effect of recombinant IL-22 on total MLKL protein expression by T2DM mice lung macrophages stimulated with  $\gamma$ -irradiated *Mtb*.** Lung macrophages were isolated from control and T2DM C57BL/6 female mice (two groups of age-matched mice). The cells were cultured with or without 10  $\mu$ g/ml  $\gamma$ -*Mtb* and in the presence or absence of recombinant IL-22 (10 ng/ml) for 72 hours. After 72 hours the supernatants were removed and the protein was extracted as mentioned in methods section. Western blot was performed to determine the expression of total MLKL levels in three independent experiments (n = 3) (**A**). Protein levels were then normalized with the level of total MLKL and  $\beta$ -actin (**B** and **C**). Pooled cells from three mice per group were used for each experiment. Statistically significant *p*-value was set at < 0.05.



## VITA

After graduating from University of Cape Coast, Ghana in 2014 with a Doctor of Optometry qualification and passing the professional licensure exams, Bismark Owusu-Afriyie worked in Ghana as a clinical optometrist for two years and moved to continue his clinical practice in Harare, Zimbabwe. He was also a part-time lecturer for anterior and posterior segment eye diseases at Bindura University of Science Education in Zimbabwe. Bismark further served as a member of the Optometry Advisory Board for the university and as the secretary of the Professional Development Committee of the Zimbabwe Optometric Association. He later joined The Fred Hollows Foundation New Zealand as a teaching optometrist in January 2020. His work station was at Divine Word University in Madang, Papua New Guinea. During this period, Bismark Owusu-Afriyie trained ophthalmic clinicians, supervised clinical students and engaged in research. In August 2021, he entered into the Biotechnology graduate program at the University of Texas at Tyler Health Science Center where he performed his thesis work in the lab of Ramakrishna Vankayalapati, Ph.D. Bismark received his Master of Science in Biotechnology degree in May 2023 and has been accepted into Ph.D. Vision Science at the University of Houston, Houston, TX to begin August 2023.

*This thesis was typed by Bismark Owusu-Afriyie*